Pergamon

Geochimica et Cosmochimica Acta, Vol. 65, No. 15, pp. 2469–2485, 2001

0016-7037/01 $20.00 + .00

PII S0016-7037(01)00603-2

The geological water cycle and the evolution of marine $\delta^{18}O$ values

K. WALLMANN*
GEOMAR-Research Center, Wischhofstr. 1-3, D-24148 Kiel, Germany

(*Received July* 13, 2000; *accepted in revised form February* 19, 2001)

Abstract—The turnover of water and ^{18}O in the outer terrestrial sphere is investigated considering mantle degassing, subduction zone processes, hydrothermal circulation at spreading centers, seafloor alteration, and continental weathering processes. Mass balances indicate that the ocean currently loses water to the mantle because the water emission by mantle degassing proceeds at a significantly slower rate than the subduction of water structurally bound in the down-going slab. The current input of ^{18}O into the ocean through hydrothermal circulation and water emissions at arc volcanoes surpasses the fixation of ^{18}O via low-temperature water/rock interactions at the seafloor and on continents, inducing an increase in marine $\delta^{18}O$ values. Results of a box model simulating the Phanerozoic water and ^{18}O cycles suggest that the mass of seawater decreased significantly causing a continuous drop in global sea-level by several hundred meters over the Phanerozoic. Model results and mass balances also allow for an enhanced estimate of current water fluxes in subduction zones consistent with the secular changes in sea-level and marine $\delta^{18}O$ observed in the geological record. Moreover, the model generates a secular trend for seawater $\delta^{18}O$—produced by the surplus of ^{18}O inputs and through internal feed-backs associated with isotopic exchange reactions at the seafloor—comparable to that observed in Phanerozoic carbonates. This coincidence suggests that the marine carbonates record a continuous change in isotopic composition of seawater with superimposed temperature-related fluctuations. A continuous record of near-surface temperatures was calculated using the model curve for seawater $\delta^{18}O$ and the corresponding carbonate data. This new climate record indicates three icehouse-greenhouse cycles with a duration of 127 My between the Cambrian and the Triassic followed by an additional cycle with extended periodicity spanning the Jurassic to Cenozoic. Simulations of the Precambrian water and ^{18}O cycles imply that the strong ^{18}O depletion in seawater during the early Cambrian ($\delta^{18}O$ around -8 ‰) was caused by enhanced weathering, diminished hydrothermal activity and extreme glaciations during the preceding late Neoproterozoic. *Copyright © 2001 Elsevier Science Ltd*

1. INTRODUCTION

Most Paleozoic and older fossils, as well as carbonate, chert and phosphate sediments are considerably lower in $\delta^{18}O$ than modern analogues (Degens and Epstein, 1962; Veizer and Hoefs, 1976). This well documented fact could be explained by diagenetic alteration, by an ^{18}O depleted ancient ocean or could indicate high surface temperatures during the early Phanerozoic. Recent compilations based on carefully selected marine fossils characterized by an excellent preservation of the ultrastructure and a minimum of diagenetic alteration (Veizer, 1995; Veizer et al., 1997; 1999) reveal a continuous increase in $\delta^{18}O$ from -8 ‰ (SMOW) during the early Cambrian to the present value (0 ‰). On this secular trend are superimposed regular oscillations, where maxima correlate with independently reconstructed cold episodes and glaciations (Veizer et al., 1999; 2000). As low temperatures favor the ^{18}O uptake in carbonates and other authigenic phases, the correlation between high ^{18}O contents and glacial conditions suggests that the marine fossil $\delta^{18}O$ record reflects both a continuous increase of seawater $\delta^{18}O$ values as well as changing surface temperatures (see also Lécuyer and Allemand, 1999). It could thus be used as an outstanding archive for the reconstruction of surface temperatures throughout the Phanerozoic if the enigmatic increase in seawater values could be explained in terms of geochemical cycles.

The $^{18}O/^{16}O$ composition of ancient oceans is one of the most controversial issues of isotope geochemistry (Land, 1995; Land and Lynch, 1999; Veizer, 1995; 1999). Most models of the geological ^{18}O cycle conclude that the $\delta^{18}O$ value of seawater is well buffered by seawater/rock interactions at the deep-sea floor as well as through continental weathering and recycling of subducted water (Muehlenbachs, 1986; 1998; Muehlenbachs and Clayton, 1976). As the oceanic crust has a constant isotopic composition and is continuously renewed through seafloor spreading and subduction, the high and low temperature reactions between seawater and oceanic basement balance externally induced $\delta^{18}O$ fluctuations and might thus maintain constant seawater composition through time (Gregory, 1991; Gregory and Taylor, 1981; Holland, 1984; Jean-Baptiste et al., 1997). In contrast, Walker and Lohmann (1989), Lécuyer and Allemand (1999), Veizer et al. (1999) and Goddéris and Veizer (2000) emphasized that the modes of water/rock interactions could change through time and could induce persistent changes in seawater composition. Thus, increasing the proportion of high-temperature processes at midocean ridges would enhance the ^{18}O content of seawater whereas an intensification of low-temperature seafloor alteration and continental weathering would decrease the marine $\delta^{18}O$ values. As the sea contains a large pool of water, the marine $\delta^{18}O$ values react only very slowly to changing inputs so that a sudden shift in ^{18}O fluxes could induce a long-term secular trend in the isotopic composition of seawater.

In this paper, the current water fluxes and ^{18}O exchange rates

*(kwallmann@geomar.de).

are reviewed to define the global water and ^{18}O budgets. Subsequently, a model is presented and applied that simulates global water and ^{18}O cycles throughout earth's history. Finally, the resulting seawater $\delta^{18}O$ values are used to evaluate the isotopic record in marine carbonates and to estimate the evolution of low-latitude temperatures during the Phanerozoic.

2. CURRENT GLOBAL WATER AND ^{18}O FLUXES

The amount of free water (seawater, meteoric water, and ice) in the exosphere (crust, oceans, and atmosphere) is controlled by mantle degassing and the turnover of water and OH-groups bound at the surface and within the lattice structure of minerals. This structurally bound water (H_2O^+) is formed during continental weathering processes and during alteration of oceanic crust. It is released and redistributed via diagenetic, metamorphic and magmatic processes at subduction zones and other tectonic settings.

The turnover of ^{18}O is related to the release and fixation of water and to isotopic exchange reactions. For mass balance purposes, the ^{18}O fluxes associated with the turnover of water are calculated from the difference between the isotopic composition of average seawater (+0 ‰) and the reacting water. In this calculation, the $\delta^{18}O$ values defined as:

$$\delta^{18}O_{SMOW} = \left(\frac{R}{R_{SMOW}} - 1\right) \cdot 1000 \quad (1)$$

are converted into ^{18}O mole fractions (Φ) using the following equation:

$$\Phi = \frac{^{18}O}{^{16}O + {}^{18}O} = \frac{R}{1+R} = \frac{R_{SMOW} \cdot \left(\frac{\delta^{18}O}{1000} + 1\right)}{1 + R_{SMOW} \cdot \left(\frac{\delta^{18}O}{1000} + 1\right)} \quad (2)$$

where R is the $^{18}O/^{16}O$ isotopic ratio and R_{SMOW} is the $^{18}O/^{16}O$ ratio in standard mean ocean water (R_{SMOW} = 0.0020052; Hoefs, 1997). The isotope ^{17}O that has a very low abundance (0.0375% of total O; Hoefs, 1997) is neglected in the calculation of ^{18}O mole fractions. The difference in $\delta^{18}O$ is converted into a difference of mole fractions and the water fluxes are multiplied with this value to calculate the net ^{18}O turnover. The ^{18}O fluxes associated with isotopic exchange reactions are calculated from the total turnover of solids during alteration and weathering taking into consideration the difference in ^{18}O mole fractions between the reacting solids (e.g., fresh oceanic crust or magmatic rocks) and resulting solid products (e.g., altered oceanic crust or clay minerals).

In the subsequent text, current fluxes in the global water and ^{18}O cycles are reviewed and critically discussed; the resulting H_2O and ^{18}O fluxes are summarized in Tables 1 and 2.

2.1. Mantle Degassing

Submarine volcanism is probably not an important source of free water because most of the released mantle water is dissolved in the basaltic matrix and only a minor fraction is emitted as gas or liquid (Javoy and Pineau, 1991; Le Cloarec and Marty, 1991). The analysis of fresh midocean ridge basalts suggests an average H_2O content of upper crust close to 0.2 wt% (Alt et al., 1996; Moore, 1970; Staudigel et al., 1996). Considering the total crust production rate at spreading centers ($5.8 \times 10^{+22}$ g My^{-1}), the resulting water flux from the mantle to the oceanic crust is $6 \times 10^{+18}$ mole H_2O My^{-1}. In contrast, subaerial volcanism releases water into the atmosphere because only a minor volatile fraction is dissolved in the volcanic solids. Assuming that mantle melts at volcanic arcs and intraplate volcanoes have a water content similar to that at midocean ridges (0.2 wt-%), the total magma production rate of subaerial volcanism (10.2 km^3 y^{-1}; Schmincke, 2000) suggests a release of $3 \times 10^{+18}$ mole H_2O My^{-1} from the mantle into the atmosphere through subaerial volcanism. The corresponding net ^{18}O fluxes from the mantle into oceanic crust and atmosphere (Table 2) are calculated from the average $\delta^{18}O$ value of mantle water (+7 ‰; Shanks et al., 1995) and the corresponding seawater value. Additional H_2O and ^{18}O fluxes at arc volcanoes induced by the recycling of subducted water are discussed in a later paragraph (section 2. 4.).

Table 1. Current water fluxes (in 10^{+18} mole My^{-1}) and isotopic signatures (‰ SMOW) at subduction zones. Numbers in brackets refer to fluxes derived from the box model (section 4.1).

Inputs into deep-sea trenches	Water Fluxes	$\delta^{18}O$
Pore water in sediments	60–100	−2
Structurally bound water (H_2O^+) in sediments	5	+17
Pore water in upper oceanic crust (0–0.5 km)	4	−1
H_2O^+ in upper oceanic crust	6	+10
H_2O^+ in deep oceanic crust (0.5–7 km) and peridotites	20–70 (≤20)	0
Mantle-H_2O^+ in oceanic crust	6	+7
Outputs into ocean, atmosphere, and mantle		
Submarine water reflux (diffuse, cold vents, mud volcanoes)	60–100	−1
Recycling through arc volcanoes	8–67 (≤21)	+10
Mantle degassing	2–3	+7
Subduction into the mantle (>250 km depth)	9–23 (≤20)	+7

2.2. Alteration of Oceanic Crust

The water content of oceanic crust is enhanced through high- and low-temperature hydrothermal processes. The current H_2O^+ formation at spreading centers can be estimated from alteration studies at DSDP/ODP Holes 896A and 504B where young oceanic crust (6–7 My) was repeatedly recovered and analyzed during the last decades (Alt et al., 1986; 1996). The average H_2O^+ content (1.3 ± 0.3 wt-%) in the upper layer (0–300 m) reflects the initial water content of fresh basalts (0.2%) and the water uptake during seafloor alteration at midocean ridges and ridge flanks (Alt et al., 1996). The alteration of early Cretaceous (120 My) upper crust was thoroughly studied at DSDP sites 417 and 418 (Fig. 1). Here, the upper crust (0–500 m) is enriched in water with an average H_2O^+-uptake of 2.8 wt-% due to pervasive contact with seawater (Staudigel et al., 1996). The high water content in the early Cretaceous crust is documented also in the metamorphic

Table 2. Current ^{18}O budget of the ocean. Numbers in brackets refer to fluxes derived from the box model (section 4.1).

Inputs in 10^{+15} mole My^{-1}		Outputs in 10^{+15} mole My^{-1}	
Isotopic exchange during high temperature seafloor alteration	2.8	Water fixation in upper oceanic crust	0.1
Water recycling at subduction zones	0.0−1.1 (0.2)	Isotopic exchange during low temperature seafloor alteration	0.9
Mantle degassing at subaerial volcanoes	0.04	Water fixation in weathering products (clay minerals)	0.2
		Isotopic exchange during continental weathering	1.4
Total	2.8–3.9 (3.0)	Total	2.6

Catalina Schists that contain water-bearing blueschists of basaltic origin (Bebout, 1996). Jurassic oceanic crust (165 My) with enhanced water contents was drilled at Hole 801 (Alt et al., 1992), confirming that old oceanic crust (>120 My) contains significantly more H_2O^+ than the young crust (6–7 My). The elevated water content of early Cretaceous and Jurassic upper crust could either be caused by continued low-temperature interactions between basalts and seawater or could reflect higher water uptake rates during the Mesozoic. More in-depth studies of the water content in an intermediate aged oceanic crust (7–120 My) are needed to investigate the dynamics of low-temperature water uptake processes. Here, we will use the data from DSDP sites 417 and 418 to define the water and the ^{18}O uptake in upper crust since these sites are well studied and often used as reference sites for the alteration of the volcanic section (Alt and Teagle, 1999; Staudigel et al., 1990; 1995; 1996). Considering the production rate ($3.6 \times 10^{+15}$ g y^{-1}; Staudigel et al., 1996) of the upper crust (0–500 m), the resulting water fixation is $5.6 \times 10^{+18}$ mole My^{-1}.

The sheeted dike complex underlying the upper basaltic layer of the oceanic crust has been extensively studied at deep-sea drilling hole 504B (Alt et al., 1986; 1995; Bach et al., 1996) where the average water content was found to be close to 1.5 wt-% (Fig. 1). The gabbro layer that extends to a depth of 7 km was never completely recovered during deep-sea drilling. A continuous section of only 500 m (Hart et al., 1999; Kempton et al., 1991; Stakes et al., 1991; Vanko and Stakes, 1991) and some samples from the deep-sea floor (e.g., Agrinier et al., 1995b) were analyzed and these showed a rather low degree of hydrothermal alteration and limited water uptake (Fig. 1). Peacock (1990) proposed an average gabbroic water content of 1 wt-% based on the sparse deep-sea and ophiolite evidence. Considering a lower crust composed of a 1.5 km thick sheeted dike complex and a 5 km thick gabbro layer, the production rate ($5.6 \times 10^{+22}$ g My^{-1}) as well as the initial (0.2 wt-%) and final (1.5 wt-% and 1 wt-% for dikes and gabbros) water contents suggest a water uptake of $28 \times 10^{+18}$ mole My^{-1}. This value should be regarded as an upper limit because the deeper gabbro layers may be essentially water-free (Fig. 1). Hydrothermal circulation is not limited to the oceanic crust but penetrates also into the underlying mantle peridotites at spreading centers, transform faults and fracture zones, to form water-bearing serpentinites at temperatures of 300°C to 500°C (Agrinier et al., 1995b; Cannat et al., 1992; Kelley, 1996; Seyfried and Dibble Jr., 1980; Snow and Dick, 1995). This process produces methane plumes in the water column that have been observed along the whole Mid-Atlantic Ridge and other tectonically active regions of the deep-sea floor indicating a widespread occurrence of serpentinite formation (Charlou et al., 1998). The total water uptake in serpentinized mantle peridotites is currently unknown. Schmidt and Poli (1998) assumed that up to $35 \times 10^{+18}$ mole H_2O My^{-1} may be fixed through this high-temperature seawater-rock interaction. The total water uptake in deep crust (>0.5 km) and peridotites probably falls into the range of 20 to $70 \times 10^{+18}$ mole H_2O My^{-1}.

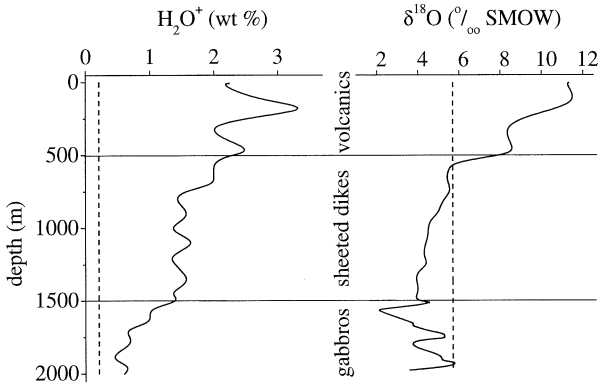

Fig. 1. Schematic depth profiles of structurally bound water (H_2O^+) and $\delta^{18}O$ in altered oceanic crust. The composite profiles are based on data obtained at different deep-sea drilling sites. The upper volcanic section (0–500 m depth) is represented by holes 417D and 418A (Staudigel et al., 1996), the sheeted dike complex was drilled at hole 504B (Alt et al., 1986; 1995; Bach et al., 1996) and the gabbros were sampled and analyzed at hole 735B (Hart et al., 1999; Robinson et al., 1991; Stakes et al., 1991). Dashed vertical lines indicate the H_2O^+ content (0.2 wt-%) and $\delta^{18}O$ value (+5.7‰) in fresh oceanic crust.

The $\delta^{18}O$ values in the upper oceanic crust (0–500 m) are significantly enhanced during low-temperature seafloor alteration processes as the resulting mineral phases, such as clays and other phyllosilicates, are enriched in the heavy isotope with respect to fresh oceanic crust ($\delta^{18}O = +5.7$ ‰,). Usually, a good correlation between H_2O^+ content and $\delta^{18}O$ values is observed in strongly altered crust suggesting that water uptake in secondary minerals has a significant impact on the isotopic composition of altered crust (Alt et al., 1992; Staudigel et al., 1995). The analysis of individual veins and samples almost completely composed of secondary silicates indicates a $\delta^{18}O$ range of +10 ‰ to +20 ‰, consistent with equilibrium isotopic fractionation at low temperatures (0–50°C; Hoefs, 1997).

The uptake of ^{18}O during seafloor alteration is related to fixation of H_2O^+ and to isotopic exchange reactions. Considering only the ^{18}O surplus with respect to seawater (+0 versus +10 ‰), the H_2O^+ formation in the upper crust ($5.6 \times 10^{+18}$ mole My^{-1}) is associated with a net ^{18}O uptake of $0.1 \times 10^{+15}$ mole ^{18}O My^{-1}. The ^{18}O uptake through isotopic exchange results from the production rate of upper crust ($3.6 \times 10^{+21}$ g

My^{-1}), the oxygen content (46 wt %), and the difference between initial and final $\delta^{18}O$ values (+5.7 and +10 ‰; Staudigel et al., 1996), and is estimated as $0.9 \times 10^{+15}$ mole $^{18}O\ My^{-1}$.

The isotopic signature of alteration products in the deep crust as well as thermodynamic data show that water-bearing phases formed by hydrothermal alteration at high temperatures (≥350°C) are depleted in ^{18}O (Bowers and Taylor, 1985; Gregory and Taylor, 1981). The sheeted dike complex underlying the upper basaltic layer of the oceanic crust is characterized by variable $\delta^{18}O$ values (+3 to +8 ‰) that indicate both ^{18}O depletion as observed at hole 504B (Fig. 1) and ^{18}O enrichments as measured in various ophiolites (Gregory and Taylor, 1981; Lécuyer and Allemand, 1999; Muehlenbachs, 1986). The $\delta^{18}O$ values decrease downward in the dikes because the temperatures of hydrothermal alteration increase with depth (Agrinier et al., 1995a; Alt et al., 1995). The underlying gabbro layer that makes up two thirds of the oceanic crust is depleted in ^{18}O (+2 to +6 ‰) due to high-temperature (>350°C) fluid-rock interactions (Hart et al., 1999; Muehlenbachs, 1986). In the lower dikes and gabbro sections, the ^{18}O depletion is controlled by the extent of hydrothermal alteration and the water/rock ratios (Alt et al., 1995; Stakes et al., 1991). Serpentinized peridotites formed at elevated temperatures are depleted in ^{18}O as well (Agrinier et al., 1995b) and thus contribute to the ^{18}O enrichment of hydrothermal fluids and to the ^{18}O transfer into the ocean. The total rate of ^{18}O release in high-temperature rock/water interactions cannot be calculated from $\delta^{18}O$ values in oceanic crust because samples from the deep crust are sparse and inhomogeneous in their isotopic composition.

In contrast, high-temperature hydrothermal fluids offer an opportunity to constrain the total ^{18}O flux into the ocean because the isotopic composition and circulation rates reflecting the reactions in deeper parts of the oceanic crust are relatively well known. Thermodynamic data suggest that H_2O^+ uptake at high temperatures (>350°C) is associated with a very small isotopic fractionation with respect to the seawater value (0 ‰). Thus, the observed enrichment of ^{18}O in high-temperature fluids (+1.1 ‰; Jean-Baptiste et al., 1997) is mainly due to isotopic exchange reactions. The total rate of ^{18}O input into the ocean through high-temperature isotopic exchange between deep rocks (crust and underlying peridotites) and seawater is estimated as $2.8 \times 10^{+15}$ mole $^{18}O\ My^{-1}$ based on the total circulation rate of high-temperature fluids at spreading centers as derived from ^3He and heat flux data ($1.3 \times 10^{+21}$ mole $H_2O\ My^{-1}$; Kadko et al., 1995; Lupton et al., 1989). Simple mass balance calculations indicate that the observed hydrothermal fluxes decrease the average $\delta^{18}O$ value of deep crust (0.5–7 km) to about +4.8 ‰ which is close to the value observed in deep-sea drilling (Fig. 1).

The ^{18}O uptake during low-temperature seafloor alteration ($1.0 \times 10^{+15}$ mole $^{18}O\ My^{-1}$) and the ^{18}O release at high temperatures ($2.8 \times 10^{+15}$ mole $^{18}O\ My^{-1}$) estimated above indicate that the water-rock interactions in the deep-sea floor produce a net increase in $\delta^{18}O$ of seawater, as previously postulated by Holland (1984) and Walker and Lohmann (1989). In contrast, model calculations and ophiolite studies suggest that the ^{18}O uptake in upper crust is balanced by the ^{18}O release from deeper crust during high-temperature basalt-seawater interactions (Bowers and Taylor, 1985; Gregory and Taylor, 1981; Muehlenbachs and Clayton, 1976).

2.3. Silicate Weathering

During weathering of igneous and high-grade metamorphic rocks on the continents, clay minerals and other H_2O^+-bearing solids are formed. The total rate of particle formation during silicate weathering can be estimated from the preindustrial suspended load of rivers. Considering that about 75% of the particles are recycled sediments (Holland, 1984; Muehlenbachs, 1998; Veizer and Jansen, 1979), the prehuman riverine particle flux to the ocean ($1 \times 10^{+22}$ g My^{-1}; Berner and Berner, 1996) and the average H_2O^+ content of weathering products (5 wt-%; Bebout, 1996; Peacock, 1990) result in a current water uptake of $7 \times 10^{+18}$ mole My^{-1}. Due to low weathering temperatures, the products of continental silicate weathering are highly enriched in the heavy ^{18}O isotope ($\delta^{18}O$ = +10 ‰ to +30 ‰; Hoefs, 1997). Thus, silicate weathering is an important sink for both H_2O and ^{18}O. Considering an average $\delta^{18}O$ value of +17 ‰ for sedimentary rocks (Li, 1972), the ^{18}O surplus with respect to free water ($\delta^{18}O$ = 0 ‰) leads to a net ^{18}O uptake of $0.2 \times 10^{+15}$ mole $^{18}O\ My^{-1}$. The ^{18}O uptake through isotopic exchange results from the production rate of particulate weathering products ($2.5 \times 10^{+21}$ g My^{-1}), the average oxygen content (50 wt %; Turekian and Wedepohl, 1961), and the difference between the initial and final $\delta^{18}O$ values (+8 ‰ for crystalline silicates; Perry and Tan, 1972; and +17 ‰ for sedimentary rocks) as $1.4 \times 10^{+15}$ mole $^{18}O\ My^{-1}$.

2.4. Water and ^{18}O Recycling at Subduction Zones

Subduction zones play a key role in the geological water cycle. Here, water bound in sediments and altered oceanic crust is either released into the exosphere or transferred into the mantle. Water enters subduction zones as porewater and chemically bound water in sediments, oceanic crust and underlying mantle peridotites and is recycled into ocean and atmosphere via submarine venting and arc volcanoes (Table 1). Using deep-sea drilling data and plate convergence rates, the input of sediment pore waters into deep-sea trenches was estimated as 1.0 to 1.8 $km^3\ y^{-1}$ (Moore and Vrolijk, 1992; Von Huene and Scholl, 1991). Sedimentary H_2O^+ is mainly found in clay minerals and biogenic opal and currently enters the deep-sea trenches at a rate of $5 \times 10^{+18}$ mole $H_2O\ My^{-1}$ (Plank and Langmuir, 1998). The inputs of H_2O^+ bound in oceanic crust and underlying peridotites correspond to the previously estimated uptake rates. In addition to these fluxes, the pore water in upper crust that constitutes about 5% of the upper crust volume (Staudigel et al., 1996) can be considered as a further water input into subduction zones (Table 1).

Porewater and H_2O^+ is recycled into the ocean through diffuse fluid flow, cold vents, mud volcanoes, and serpentine diapirs. As sediments are strongly compacted during subduction, most of the pore water is expelled into the ocean. Moreover, fore-arc pore waters sampled in deep-sea drilling cores are occasionally diluted with fresh water released during clay mineral and biogenic opal diagenesis (Kastner et al., 1993; 1990) indicating additional reflux of H_2O^+ into the ocean. Metamorphic waters from deeper strata are released through

the central conduit of deep-rooted serpentine mud volcanoes (Fryer et al., 1990). Experimental data indicate that water content of the oceanic crust is significantly reduced upon subduction so that only $25 \pm 8 \times 10^{+18}$ mole H_2O My^{-1} reach the source area of arc volcanoes below 70 to 80 km depth with the remainder released at shallower depth where it is either transferred into the ocean or into the cold corner of the mantle wedge (Schmidt and Poli, 1998). Water released into the upper mantle wedge overlying the subducted slab (cold corner) is either transported into deeper strata with the down-welling mantle where it contributes to arc volcanism, or it may rise to the surface and feed the submarine serpentine diapirs. As submarine water recycling is mainly driven by sediment compaction, the total submarine reflux is close to the pore water input flux (Table 1).

The subaerial water release at arc volcanoes can be deduced from volcanic gas analysis (Giggenbach, 1992; 1996), from experimentally based phase diagrams of hydrous basalts (Schmidt and Poli, 1998) and from mass balances (Ito et al., 1983). Using stable isotope data, Giggenbach (1992) detected a deep 'andesitic' water component in volcanic gases at convergent plate boundaries that is released from the subducted slab and occurs at an average molar H_2O/He ratio of $2.2 \times 10^{+6}$. Considering the global ^3He emission at arc volcanoes (200 mol ^3He y^{-1}; Torgersen, 1989) and the average $^3He/^4He$ ratio of volcanic arc gases (8.3×10^{-6}; Sano and Williams, 1996), the water emission can be estimated as $53 \times 10^{+18}$ mole My^{-1}. The experimental data on metamorphic water release imply that 33 to 67 $\times 10^{+18}$ mole H_2O My^{-1} are available for arc volcanism (Schmidt and Poli, 1998). These two independent and converging evaluations are significantly higher than the previous estimates based on mass balances ($8 \times 10^{+18}$ mole My^{-1}; Ito et al., 1983; Peacock, 1990). Additional data on the water content of incoming oceanic crust and the water emissions at arc volcanoes are needed to constrain better the water reflux into the atmosphere at subduction zones. An unknown portion of the incoming water is not recycled into the ocean and the atmosphere, but subducted into the mantle (Schmidt and Poli, 1998). The deep subduction of H_2O^+ is favored by low temperatures of the subducted slab (Thompson, 1992) and is most pronounced for the deeper portion of the subducted slab where H_2O^+ is sparse, and thus far from saturation (Schmidt and Poli, 1998).

The isotopic composition of water expelled at submarine cold vents and mud diapirs reflects the composition of sediment pore waters (−2 ‰) and occasional additions of isotopically enriched H_2O^+ released during diagenetic and metamorphic processes (Kastner et al., 1993). Taking an average value of −1 ‰, the formation and recycling of pore water into the ocean leads to a ^{18}O loss of about $0.2 \times 10^{+15}$ mole My^{-1}. The deep 'andesitic water' released at arc volcanoes has an average $\delta^{18}O$ value of +10 ‰ that reflects the preferential recycling of H_2O^+ from sediments and upper oceanic crust (Giggenbach, 1992). Considering the total water flux ($8-67 \times 10^{+18}$ mole My^{-1}), the surplus of ^{18}O with respect to seawater ($\delta^{18}O = 0$) amounts to a ^{18}O release of 0.16 to $1.3 \times 10^{+15}$ mole ^{18}O My^{-1}. Thus, the water recycling into ocean and atmosphere produces a net ^{18}O release of 0.0 to $1.1 \times 10^{+15}$ mole My^{-1}.

2.5. Global Water and ^{18}O Balances

The total mass of free water is determined by mantle degassing as well as the formation and recycling of H_2O^+. The oceanic crust is the largest water sink on earth so that the dewatering of subducted slabs acts as the major control on the global water mass. A general marine regression with superimposed fluctuations related to periodic changes in seafloor spreading has been observed for the Phanerozoic (Hallam, 1992). This regression either reflects a decrease in free water mass by up to 10% or a deepening of ocean basins due to a continuous slow-down of tectonic activity. The oceans currently contain about $8.1 \times 10^{+22}$ mole H_2O (Broecker and Peng, 1982). Thus, the Phanerozoic sea level change allows for a decrease in free water of $8.1 \times 10^{+21}$ mole H_2O over a period of 560 My corresponding to a net water export of $14 \times 10^{+18}$ mole My^{-1}. This modest change in global water mass suggests that the subduction of water into the mantle should proceed at an average rate of only $9-23 \times 10^{+18}$ mole My^{-1} considering the rather slow mantle degassing ($3 \times 10^{+18}$ mole My^{-1}) and the subduction of primary mantle-H_2O^+ bound in oceanic crust ($6 \times 10^{+18}$ mole My^{-1}).

The ^{18}O fluxes summarized in Table 2 imply that the $\delta^{18}O$ value of seawater is currently not at steady state but is increasing because the release of ^{18}O at spreading centers and subduction zones is not balanced by ^{18}O uptake through continental silicate weathering and by alteration processes at the deep-sea floor. The largest ^{18}O input into the ocean is generated through high-temperature fluids at spreading centers. Recently, Jean-Baptiste et al. (1997) proposed an even higher ^{18}O input through hydrothermal fluids that would further enhance the ^{18}O imbalance. Thus, the hydrothermal ^{18}O input listed in Table 2 is in fact a conservative estimate and should not be revised to a lower value. The ^{18}O consumption through silicate weathering is the main sink for oceanic ^{18}O in the model. The adopted flux is higher than the previously published values (Holland, 1984; Muehlenbachs, 1986; 1998; Muehlenbachs and Clayton, 1976). Diminishing this estimate to lower weathering rates would again enhance the ^{18}O imbalance and could therefore not solve the budget problem. Low-temperature seafloor alteration is the other important mechanism for ^{18}O removal. The current flux is based on studies in strongly altered Cretaceous crust (Staudigel et al., 1996) that contains significantly more water and ^{18}O than oceanic crust drilled at other locations (Alt, 1993; Alt et al., 1986; 1996). Thus, an upward revision would not be consistent with deep-sea drilling data. The ^{18}O release through water recycling at subduction zones could fall into the lower range of previous estimates. It is possible that only a small fraction of H_2O^+ bound in deeper strata of the subducted slab (gabbros and underlying peridotites) is emitted through arc volcanoes into atmosphere and ocean whereas the dominant portion is subducted into the mantle. These deeper layers contain considerable amounts of H_2O^+ dispersed over a very large mass of oceanic crust and mantle rocks. The resulting low H_2O^+ concentration hinders an efficient recycling because H_2O^+ is tightly bound in undersaturated rocks (Schmidt and Poli, 1998). Recently, growing number of mineral phases was identified and experimentally investigated that could carry the remaining H_2O^+ into the mantle (Bose and Navreotsky, 1998; Chinnery et al., 1999; Liu and Bohlen, 1996; Mysen and Acton,

Table 3. Water fluxes and ^{18}O turnover considered in the box model.

Flux	Equation
H_2O fixation in weathering products	$F_w = f_{sp} \cdot F_w(0)$
H_2O uptake in upper crust (0–500 m)	$F_{alt} = f_{sp} \cdot F_{alt}(0)$
H_2O uptake in deep crust (>0.5 km)	$F_{sp} = f_{sp} \cdot F_{sp}(0)$
H_2O release from weathering products	$F_{rew} = r_w \cdot F_w$
H_2O release from upper crust at subduction zones	$F_{reup} = r_{up} \cdot F_{alt}$
H_2O release from deep crust at subduction zones	$F_{redeep} = r_{deep} \cdot F_{sp}$
H_2O release through mantle degassing	$F_m = f_{sp} \cdot F_m(0)$
$H_2{}^{18}O$ uptake in continental weathering products	$F_w^{18} = \frac{\alpha_w \cdot R_f}{1 + \alpha_w \cdot R_f} \cdot F_w$
$H_2{}^{18}O$ uptake in upper crust (0–500 m)	$F_{alt}^{18} = \frac{\alpha_{up} \cdot R_f}{1 + \alpha_{up} \cdot R_f} \cdot F_{alt}$
$H_2{}^{18}O$ uptake in deep crust (>0.5 km)	$F_{sp}^{18} = \frac{\alpha_{deep} \cdot R_f}{1 + \alpha_{deep} \cdot R_f} \cdot F_{sp}$
^{18}O exchange during weathering	$F_w^{ex} = f_{sp} \cdot k_w \cdot (\Omega_w - 1)$
^{18}O exchange between upper crust and seawater	$F_{up}^{ex} = f_{sp} \cdot k_{up} \cdot (\Omega_{up} - 1)$
^{18}O exchange between deep crust and seawater	$F_{deep}^{ex} = f_{sp} \cdot k_{deep} \cdot (\Omega_{deep} - 1)$
^{18}O loss during porewater formation and recycling	$F_{pw}^{18} = f_{sp} \cdot F_{pw}^{18}(0)$
$H_2{}^{18}O$ release from weathering products	$F_{rew}^{18} = \Phi_w \cdot F_{rew}$
$H_2{}^{18}O$ release from upper crust at subduction zones	$F_{reup}^{18} = \Phi_{up} \cdot F_{reup}$
$H_2{}^{18}O$ release from deep crust at subduction zones	$F_{redeep}^{18} = \Phi_{deep} \cdot F_{redeep}$
$H_2{}^{18}O$ release through mantle degassing	$F_m^{18} = \Phi_m \cdot F_m$
formation of sedimentary rock ^{18}O	$F_{ps}^{18} = \Phi_{si} \cdot f_{sp} \cdot F_{ps}(0)$
formation of upper crust ^{18}O at spreading zones	$F_{pup}^{18} = \Phi_{oc} \cdot f_{sp} \cdot F_{pup}(0)$
formation of deep crust ^{18}O at spreading zones	$f_{pdeep}^{18} = \Phi_{oc} \cdot f_{sp} \cdot F_{pdeep}(0)$
metamorphosis of sedimentary rock ^{18}O	$F_{ms}^{18} = \Phi_w \cdot f_{sp} \cdot F_{ps}(0) + \Phi_w \cdot (1 - r_w) \cdot F_w$
subduction of upper crust ^{18}O	$F_{sup}^{18} = \Phi_{up} \cdot f_{sp} \cdot F_{pup}(0) + \Phi_{up} \cdot (1 - r_{up}) \cdot F_{alt}$
subduction of deep crust	$F_{sdeep}^{18} = \Phi_{deep} \cdot f_{sp} \cdot F_{pdeep}(0) + \Phi_{deep} \cdot (1 - r_{deep}) \cdot F_{sp}$

1999; Ono, 1998; Ulmer and Trommersdorff, 1995). Moreover, released water can leave the slab only through an interconnected network of fluid-filled grain boundaries or micro-fractures. The incomplete wetting of mineral grain boundaries in water-poor rocks could hinder the build-up of a fluid network so that the released water is trapped as interstitial fluid in subducting gabbros and mantle peridotites (Mibe et al., 1999; Watson and Lupulescu, 1993).

Secular trends in the isotopic composition of marine carbonates can be used to constrain possible changes in seawater ^{18}O and the magnitude of current ^{18}O fluxes using the dynamic model of water and ^{18}O cycling presented and applied in the following sections. It is not possible to derive exact flux values from simple isotope balances because changes in isotopic composition over the Phanerozoic are likely to be non-linear due to variable tectonic/volcanic activities and internal feed-backs.

3. A NEW BOX MODEL FOR GLOBAL WATER CYCLING AND ^{18}O TURNOVER

A new box model is presented and applied to investigate the evolution of water masses and seawater ^{18}O values throughout earth's history. The water model considers the formation and recycling of H_2O^+ and the release of water from the mantle. The fluxes are defined by the current fluxes attenuated by the Phanerozoic spreading rates previously reconstructed and applied by Berner (1994). These non-dimensional rates (f_{sp}) represent the relative changes in tectonic and volcanic activity normalized to the current value. The recycling fluxes are related to the fixation of H_2O^+ and to a recycling efficiency (r) that defines the portion of H_2O^+ released through diagenesis and metamorphism at subduction zones and in other tectonic settings. The change in free water mass is controlled by the recycling efficiency. The fixation of mantle water in oceanic crust and the subduction of mantle-H_2O^+ are not considered presuming that these two fluxes are balanced. Sheeted dikes, gabbros and peridotites are summarized as "deep crust" and it is assumed that this deep crust reacts with seawater only at high temperatures (>350°C). Water fluxes, the mass balance of free water through time as well as all constant and time-dependent parameter values are summarized in Tables 3 to 6.

The isotopic composition of free water is affected by the turnover of H_2O^+ and by isotopic exchange processes with oceanic crust and continental silicate rocks. The isotopic exchange between seawater and oceanic crust is a key process in the evolution of the marine $\delta^{18}O$ values as it tends to stabilize the seawater composition through interactions with the large and constantly renewed pool of oceanic crust. The exchange process is driven by thermodynamic forces and proceeds through surface diffusion, dissolution of fresh crust minerals and precipitation of alteration products. The thermodynamic control can be expressed using a saturation index Ω:

Table 4. Mass balances for free water and ^{18}O used in the box model.

Reservoir	Differential equation
Change in free H_2O mass	$\frac{dM_f}{dt} = F_{rew} + F_{reup} + F_{redeep} + F_m - F_w - F_{alt} - F_{sp}$
Change in free $H_2{}^{18}O$ mass	$\frac{dM_f^{18}}{dt} = F_{rew}^{18} + F_{reup}^{18} + F_{redeep}^{18} + F_m^{18} + F_w^{ex} + F_{up}^{ex} + F_{deep}^{ex} - F_w^{18} - F_{alt}^{18} - F_{sp}^{18} - F_{pw}^{18}$
Change in ^{18}O mass in sedimentary rocks	$\frac{dM_w^{18}}{dt} = F_{ps}^{18} + F_w^{18} + F_{pw}^{18} - F_w^{ex} - F_{rew}^{18} - F_{ms}^{18}$
Change in ^{18}O mass in upper crust	$\frac{dM_{up}^{18}}{dt} = F_{pup}^{18} + F_{alt}^{18} - F_{up}^{ex} - F_{reup}^{18} - F_{sup}^{18}$
Change in ^{18}O mass in deep crust	$\frac{dM_{deep}^{18}}{dt} = F_{pdeep}^{18} + F_{sp}^{18} - F_{deep}^{ex} - F_{redeep}^{18} - F_{sdeep}^{18}$

$$\Omega = \frac{R/R_f}{\alpha} \tag{3}$$

where R and R_f are $^{18}O/^{16}O$ ratios in fresh oceanic crust and seawater, respectively, and α is the isotopic fractionation factor for H_2O — crust interactions ($\alpha = R/R_f$ at equilibrium). The rate of isotopic exchange is

$$F^{ex} = f_{sp} \cdot k \cdot (\Omega - 1) \tag{4}$$

where f_{sp} is the spreading rate and k is a kinetic constant that describes the efficiency of the dissolution/precipitation processes. At isotopic equilibrium, Ω is unity and the net rate of isotopic exchange is zero. With the actual ratios R/R_f smaller than the equilibrium value α, the isotopic exchange takes a negative sign and ^{18}O is released from the crust into seawater. In contrast, ^{18}O is transferred into the crust when the actual ratio is greater than at equilibrium (e.g., $R/R_f > \alpha_{oc}$, $\Omega > 1$). As the isotopic composition of fresh oceanic crust is constant through time, changes in seawater composition define the direction and the intensity of the exchange reactions. Close to isotopic equilibrium, the exchange rates are diminished whereas large deviations from equilibrium produce strong isotopic exchange fluxes. This response of exchange rate to the extent of disequilibrium exerts a strong stabilizing effect on the isotopic composition of seawater. On the other hand, the isotopic exchange is controlled by the rates of chemical dissolution and precipitation processes that lead to seafloor alteration. This chemical control on isotopic exchange and seawater composition is expressed by the kinetic constant k that can vary through time. Through this formulation of isotopic exchange (Eqn. 4) both the isotopic buffering of seawater by water—rock interactions (Holland, 1984; Jean-Baptiste et al., 1997; Muehlenbachs and Clayton, 1976) as well as possible changes in seawater composition via enhanced high- or low-temperature reactions (Walker and Lohmann, 1989) are considered and can thus be simulated in the model. Eqn. 4 should not be confused with kinetic equations that describe the isotopic exchange processes at the molecular level (e.g., Cole and Ohmoto, 1986;

Table 5. Constant parameter values used in the definition of model fluxes.

Parameter	Symbol/Value
Current H_2O fixation in weathering products	$F_w(0) = 7 \times 10^{+18}$ mole My^{-1}
Current H_2O fixation in upper crust	$F_{alt}(0) = 6 \times 10^{+18}$ mole My^{-1}
Current H_2O fixation in deep crust	$F_{sp}(0) = 20 - 70 \times 10^{+18}$ mole My^{-1}
Current H_2O release from the mantle	$F_m(0) = 3 \times 10^{+18}$ mole My^{-1}
Current production of sedimentary rock oxygen	$F_{ps}(0) = 7.8 \times 10^{+19}$ mole My^{-1}
Current production of upper crust oxygen	$F_{pup}(0) = 1.2 \times 10^{+20}$ mole My^{-1}
Current production of deep crust oxygen	$F_{pdeep}(0) = 1.6 \times 10^{+21}$ mole My^{-1}
Current ^{18}O loss during turnover of porewater	$F_{pw}^{18}(0) = 2 \times 10^{+14}$ mole My^{-1}
Fraction of recycled sedimentary rock H_2O	$r_w = 1$
Fraction of recycled upper crust H_2O	$r_{up} = 1$
Fraction of recycled deep crust H_2O	$r_{deep} = 0$ to 1
Kinetic constant for isotopic exchange during weathering	$k_w = 1.2 \times 10^{+17}$ mole ^{18}O My^{-1}
Kinetic constant for isotopic exchange during alteration of upper crust	$k_{up} = 1.0 \times 10^{+17}$ mole ^{18}O My^{-1}
Kinetic constant for isotopic exchange during alteration of deep crust	$k_{deep} = 4.9 \times 10^{+17}$ mole ^{18}O My^{-1}
Isotopic fractionation factor for H_2O uptake in clays	$\alpha_w = 1.02$
Isotopic fractionation factor for H_2O uptake in upper crust	$\alpha_{up} = 1.015$
Isotopic fractionation factor for H_2O uptake in deep crust	$\alpha_{deep} = 1$
^{18}O mole fraction in weathering silicate rocks	$\Phi_{si} = 2.017 \times 10^{-3}$
^{18}O mole fraction in fresh crust	$\Phi_{oc} = 2.0126 \times 10^{-3}$
^{18}O fraction in mantle water	$\Phi_m = 2.015 \times 10^{-3}$
Mass of oxygen in sedimentary rocks	$M_w = 7 \times 10^{+22}$ mole
Mass of oxygen in upper crust (0–0.5 km)	$M_{up} = 1.0 \times 10^{+22}$ mole
Mass of oxygen in deep crust	$M_{deep} = 1.6 \times 10^{+23}$ mole

Table 6. Time-dependent model variables.

Variable	Symbol/Equation
^{18}O mole fraction in free water	$\Phi_f = M_f^{18}/M_f$
^{18}O mole fraction in sedimentary rocks	$\Phi_w = M_w^{18}/M_w$
^{18}O mole fraction in upper crust	$\Phi_{up} = M_{up}^{18}/M_{up}$
^{18}O mole fraction in deep crust	$\Phi_{deep} = M_{deep}^{18}/M_{deep}$
Corresponding $^{18}O/^{16}O$ ratios	$R = \frac{\Phi}{1-\Phi}$
Isotopic saturation index for ^{18}O exchange during silicate weathering	$\Omega_w = \frac{R_{si}/R_f}{\alpha_w}$
Isotopic saturation index for ^{18}O exchange between upper crust and seawater	$\Omega_{up} = \frac{R_{oc}/R_f}{\alpha_{up}}$
Isotopic saturation index for ^{18}O exchange between deep crust and seawater	$\Omega_{deep} = \frac{R_{oc}/R_f}{\alpha_{deep}}$

Lécuyer and Allemand, 1999) but should be regarded as a highly simplifying process formulation that relates exchange rates to the intensity of alteration and to seawater composition. Similar equations were previously used to describe dissolution of mineral phases such as biogenic opal and calcite in seawater (Hales and Emerson, 1997; Hurd, 1972).

The absolute value of kinetic constant k is calculated from the current isotopic ratios in fresh rocks and seawater ($R_f(0)$) and the current exchange flux ($F^{ex}(0)$) as:

$$k = \left| = \frac{\alpha \cdot F^{ex}(0)}{\frac{R}{R_f(0)} - \alpha} \right| \quad (5)$$

The isotopic exchange processes between weathering silicates and meteoric waters during continental weathering are formulated using the same approach (Eqn. 4). In the modelling it is assumed that the isotopic composition of the water reacting with oceanic crust and continental silicates corresponds to the composition of the total free water in the exosphere that is calculated in the model as time-dependent parameter.

The uptake of $H_2^{18}O$ in rocks depends on the total water uptake (F), the isotopic fractionation factor, and the isotopic composition of free water that changes through time:

$$F^{18} = \frac{\alpha \cdot R}{1 + \alpha \cdot R_f} \cdot F \quad (6)$$

This formulation produces an additional stabilization of the isotopic composition of free water.

The return fluxes of ^{18}O into the exosphere at subduction zones and other settings (F_{re}^{18}) depend on the isotopic composition of the H_2O^+-bearing rocks and the water release rates (F_{re}) as:

$$F_{re}^{18} = \Phi \cdot F_{re} \quad (7)$$

The ^{18}O mole fractions (Φ) are calculated for each time step taking into account the changing isotopic compositions of oceanic crust and sedimentary rocks.

The isotopic composition of upper and lower crust is maintained at a relatively constant level through continuous production of fresh crust and subduction of altered crust. The production is formulated as:

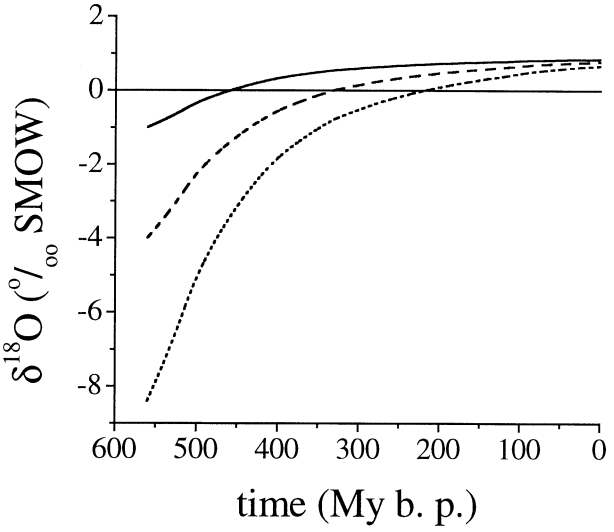

Fig. 2. Change in isotopic composition of free water through the Phanerozoic assuming high water uptake in deep crust and peridotites ($F_{sp}(0) = 63 \times 10^{+18}$ mole My^{-1}), complete recycling of H_2O^+ and different initial $\delta^{18}O$ values.

$$F_p^{18} = \Phi_{OC} \cdot f_{sp} \cdot F_p(0) \quad (8)$$

where F_p^{18} and $F_p(0)$ are the formation of crustal ^{18}O and O and Φ_{OC} is the mole fraction of ^{18}O in fresh crust. $F_p(0)$ and Φ_{OC} are constant through time. The subduction of crustal ^{18}O (F_s^{18}) follows:

$$F_s^{18} = \Phi \cdot f_{sp} \cdot (F_p(0) + F(0)) - F_{re}^{18} \quad (9)$$

where F(0) is water uptake in crust corresponding to the current value and Φ is the variable mole fraction of ^{18}O in altered crust. The complete set of fluxes, the related parameter values, and the mass balances considered in the model are listed in Tables 3 to 6.

The commercial software ModelMaker, Version 3 (Cherwell Scientific Publishing Limited) was used to implement the box model. ModelMaker solves the set of coupled first order differential equations defined in Table 4 using the numerical Runge-Kutta method (Press et al., 1992). Mass balance calculations used as a control to the model results showed that masses of free water and ^{18}O are completely conserved during numerical calculations. A typical model run was completed within a second on a PC with Pentium III processor.

4. MODEL RESULTS AND IMPLICATIONS

4.1. Modeling the Phanerozoic Water and ^{18}O Cycles

As a first application of the model, the evolution of $\delta^{18}O$ values in free water was simulated from the early Cambrian to the present assuming complete water recycling ($r_w = r_{up} = r_{deep} = 1$), a high water uptake in deep crust and peridotites ($F_{sp}(0) = 63 \times 10^{+18}$ mole My^{-1}) corresponding to previous estimates (Peacock, 1990; Schmidt and Poli, 1998) and different initial $\delta^{18}O$ values (Fig. 2). As more than 95% of the total free water in the exosphere has accumulated in the oceans, the simulated free water pool is equivalent to seawater. The lowest initial value (−8.4 ‰) corresponds to the marine carbonate

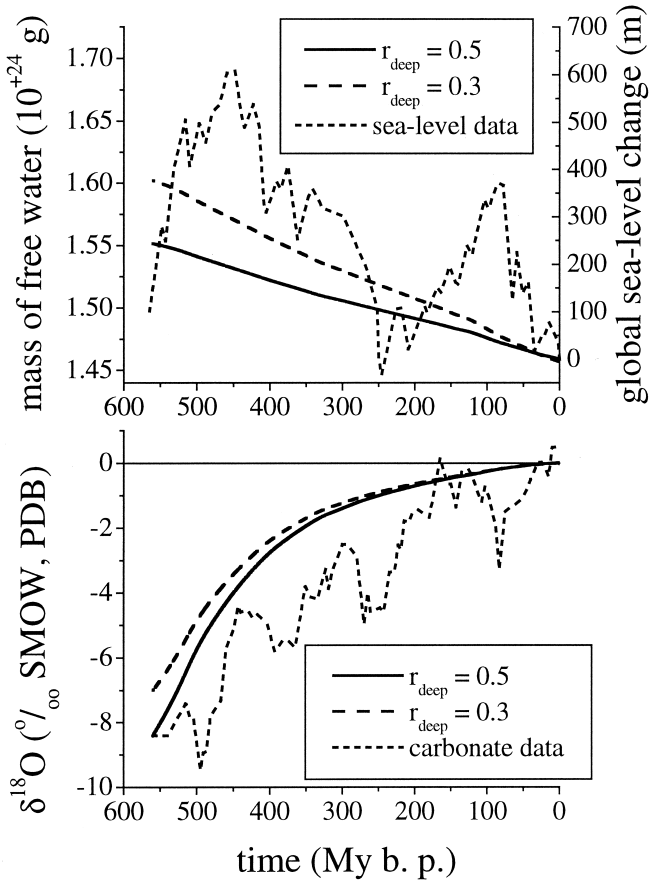

Fig. 3. Change in the mass and isotopic composition of free water. The upper diagram shows water masses calculated in two model runs and the Phanerozoic sea-level change reconstructed by Hallam (1992). A decrease in water mass by 10% corresponds to a drop in global sea-level of roughly 400 m at the current distribution of oceanic depth levels. In the lower diagram, the isotopic composition of seawater (‰ SMOW) as simulated with the box model is compared to the Phanerozoic $\delta^{18}O$ trend in marine carbonates (‰ PDB) recently compiled by Veizer et al. (1999). Solid lines indicate the results of a model run with a recycling efficiency r_{deep} of 0.5 for water bound in deep crust whereas the model results indicated by the dashed lines were calculated with $r_{deep} = 0.3$. The water uptake rate in deep crust $F_{sp}(0)$ was $20 \times 10^{+18}$ mole My^{-1} in both model runs.

value reconstructed by Veizer et al. (1999) and assumes that the carbonate fossils could record a change in seawater isotopic composition whereas the highest value (−1 ‰) represents Holocene seawater in an hypothetical ice-free world. In either case, the simulation produces a rapid increase to positive $\delta^{18}O$ values significantly higher than the current seawater value (0 ‰). These positive values are caused by the imbalance in the marine ^{18}O budget (Table 2) that was enhanced assuming strong water uptake in deep oceanic crust and complete $H_2^{18}O$ recycling at subduction zones. The above model demonstrates that a strong dominance of ^{18}O inputs into the ocean is not consistent with the evolution of the geochemical ^{18}O cycle.

Model simulations were run with a reduced water uptake in deep crust and a diminished recycling efficiency of water in deep crust ($r_{deep} < 1$) to test the impact of recycling on the evolution of water mass and marine $\delta^{18}O$ values and to constrain the recycling of H_2O^+ at subduction zones (Fig. 3). In these model runs, the initial mass and isotopic composition of free water, the current water fixation in deep crust and peridotites $F_{sp}(0)$ and the recycling efficiency r_{deep} were tuned to reproduce the current seawater mass ($1.46 \times 10^{+24}$ g) and $\delta^{18}O$ value (0 ‰). The initial values for the early Cambrian were varied within the restricted ranges of −8.4 to −1 ‰ and 1.6 to $1.46 \times 10^{+24}$ g defined by the carbonate and sea level data, respectively (section 2.5). The modeling showed that the current $\delta^{18}O$ value and water mass are obtained only with $F_{sp}(0) \leq 20 \times 10^{+18}$ mole My^{-1}, $r_{deep} = 0.3$ - 0.5 and an initial $\delta^{18}O$ value in the range of −8.4 to −7.0 ‰. These parameter values imply that less than $14 \times 10^{+18}$ mole My^{-1} of H_2O^+ bound in altered crust and serpentinized peridotites is currently subducted into the mantle. Considering the primary mantle-H_2O^+ bound in the crust, the total flux of water into the mantle is $\leq 20 \times 10^{+18}$ mole My^{-1} (Table 1). The water recycling via arc volcanoes ($F_{re}(0)$) as driven by H_2O^+ released from sediments, upper crust, deep crust and serpentinized peridotites is restricted to $\leq 21 \times 10^{+18}$ mole My^{-1} by this model result (Table 1). Considering the independent data on volcanic water emissions and crust alteration summarized in section 2, the real fluxes may be estimated as $F_{re}(0) \approx F_{sp}(0) \approx 20 \times 10^{+18}$ mole My^{-1}. With these estimates, the net ^{18}O release at subduction zone reduces to $0.2 \times 10^{+15}$ mole My^{-1}, the total ^{18}O input flux into the ocean is $3.0 \times 10^{+15}$ mole My^{-1} and

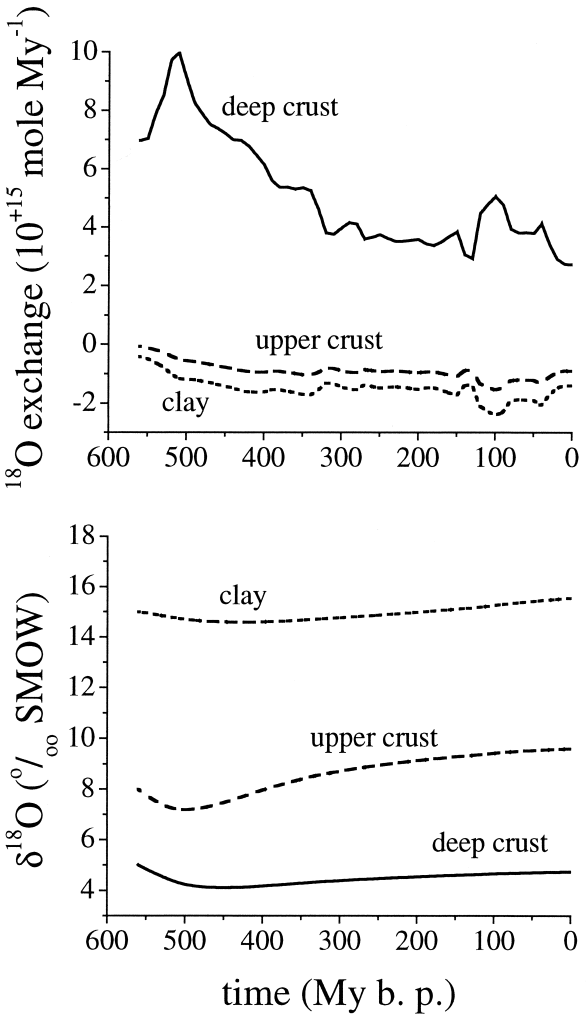

Fig. 4. Isotopic exchange fluxes and isotopic composition of deep crust, upper crust and clays throughout the Phanerozoic as simulated with the box model using $r_{deep} = 0.5$ and $F_{sp}(0) = 20 \times 10^{+18}$ mole My^{-1}.

the present surplus of ^{18}O inputs amounts to $0.4 \times 10^{+15}$ mole My^{-1} (Table 2). The residence time of free water in the exosphere with respect to the current volcanic water emissions driven by mantle degassing and H_2O^+ recycling at subduction zones results as 3.5 Gy.

Figure 4 illustrates the ^{18}O buffering of the ocean through reactions with oceanic crust. Due to the large difference between the initial δ^{18}O values in deep crust and seawater, the isotopic exchange and the ^{18}O release into the ocean through hydrothermal fluids is strongly enhanced. In contrast, the low initial $^{18}O/^{16}O$ ratio in seawater and the high ratios in oceanic crust and weathering silicate rocks almost correspond to isotopic equilibrium so that the isotopic exchange and the ^{18}O uptake through low-temperature reactions is significantly reduced. The increase in marine δ^{18}O values is accelerated during the early Phanerozoic due to these enhanced ^{18}O inputs and diminished outputs. The δ^{18}O values calculated for sedimentary rocks and oceanic crust demonstrate that the isotopic composition of sediments and crust is only weakly affected by seawater composition because the rocks are continuously renewed through erosion and weathering of crystalline silicate rocks, metamorphosis of sedimentary rocks, spreading and subduction.

In Figure 3, the marine δ^{18}O values calculated in the model are compared to the Phanerozoic isotope data in marine carbonates recently compiled by Veizer et al. (1999). The independent isotope measurements show a similar change over time as the model curve. The positive excursions from the general trend occur during periods where glaciations and cool periods are suggested by independent geologic evidence, while the negative deviations correspond to suspected greenhouse periods (Veizer et al., 1999; 2000). Only, the high ^{18}O values during the Jurassic might be inconsistent with the geological record which implies moderate temperatures for this period (Frakes et al., 1992). The rather good correspondence between the basic trend of the carbonate data and the model curves implies that the marine carbonates record a continuous change in seawater composition with a superimposed periodic signal presumably related to global climate.

Changes in global sea-level are usually attributed to changes in the volume of ocean basins and to the formation of large continental ice shields. The model results presented in Figure 3 imply an alternative explanation. They suggest that the total mass of free water in the exosphere (seawater, meteoric water and ice) has decreased considerably during the Phanerozoic causing a continuous fall in global sea-level of several hundred meters. The superimposed fluctuations are probably related to regular changes in seafloor spreading, to the build-up and break-up of large continental blocks and to continental ice formation whereas the general marine regression observed in the Phanerozoic sea-level record (Hallam, 1992) could be caused by the subduction of water bound in deep oceanic crust.

4.2. Modeling the Water and ^{18}O Cycles Throughout Earth's History

Even though the Phanerozoic increase in marine δ^{18}O values is in line with the current modes of water and ^{18}O cycling, the extremely low abundance of ^{18}O at the beginning of the Phanerozoic is not explained in the previous modeling. To address this item, the simulation of water and ^{18}O cycles is extended to include the Precambrian.

The model, as defined in Tables 3 to 6, is now used to simulate the water cycle commencing with the formation of solid earth at 4.6 Gy b. p. and ending with the current state (Fig. 5). The change in volcanic/tectonic activity (f_{sp}), needed to define various water fluxes (Table 3), was formulated according to Phipps Morgan (1998) who showed that the relative rate of mantle overturn and differentiation over earth's history is proportional to the square of heat loss. In contrast to the Phanerozoic model, the mantle degassing through volcanoes was related not only to the change in volcanic activity (f_{sp}) but also to the changing water concentration in the mantle. The water content was assumed to decay exponentially and the parameters of the exponential function were tuned to produce the final mass of free water corresponding to the current value ($1.46 \times 10^{+24}$ g). The geochemical evolution of crustal rocks indicates that subduction was accompanied by slab melting during the first 2 to 3 Gy of earth's history (Taylor and McLennan, 1995).

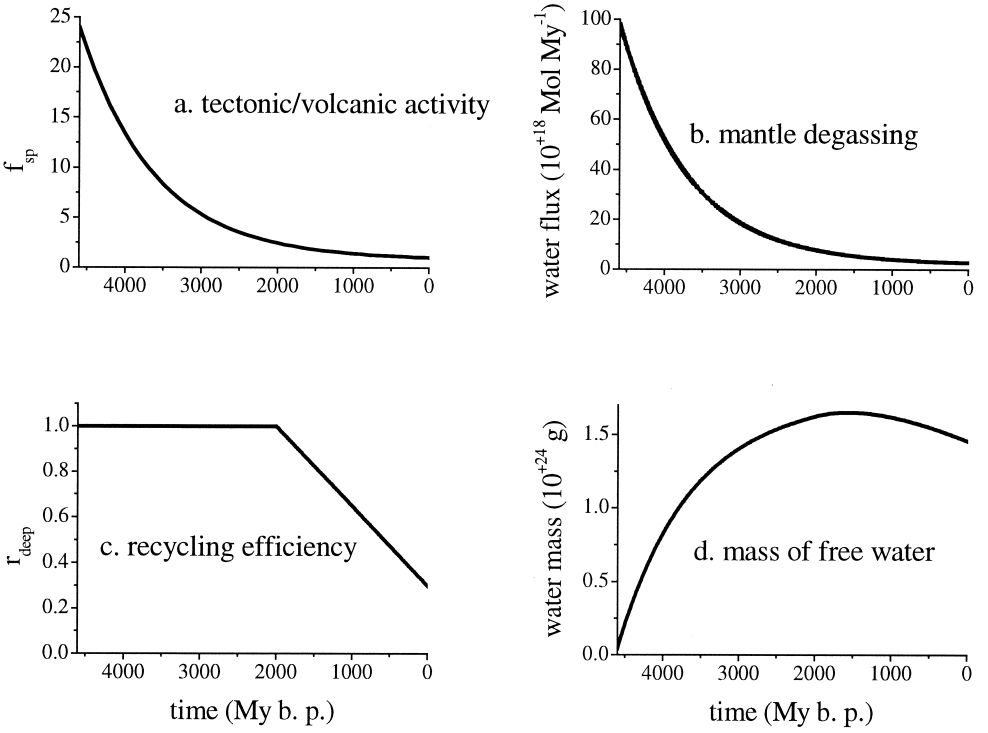

Fig. 5. Water cycling through earth's history as assumed for the simulation of marine $\delta^{18}O$ values. a. The non-dimensional tectonic/volcanic activity (f_{sp}) is taken to be proportional to the square of heat loss (Phipps Morgan, 1998). b. The water flux from the mantle is proportional to f_{sp} and to the H_2O^+ concentration in the mantle that is assumed to decay exponentially through time. The recycling efficiency of H_2O^+ bound in the deep mantle and in underlying peridotites (r_{deep}) is unity until the onset of cold subduction (Taylor and McLennan, 1995) and decreases subsequently to 0.3. d. The change in free water mass is calculated using the model fluxes listed in Tables 3 and 5 ($F_{sp}(0) = 20 \times 10^{+18}$ mole My^{-1}), with the water flux from the mantle as depicted in Figure 5b and the changing recycling efficiency shown in Figure 5c.

Cold subduction with limited water recycling occurred only during the last 2 Gy. For this reason, the recycling efficiency of water bound in the deeper portions of the subducted slab (r_{deep}) was taken as unity until the onset of cold subduction (Fig. 5). The resulting change in free water mass showed a rapid increase for the young earth followed by the development of a broad maximum and, finally, a decrease in free water after the onset of cold subduction (Fig. 5). As the parameters of the model are poorly constrained, the simulated changes in water mass should be regarded only as a first order approximation. Nevertheless, a slow decrease in free water mass is consistent with the general marine regression observed during the Phanerozoic (Hallam, 1992). The model results are also confirmed by a recent reconstruction of Proterozoic sea-level change which indicates a marine transgression from 3 Gy to 2 Gy cumulating in a strong maximum in sea-level at 1.9 Gy and followed by a marine regression continuing till 1 Gy b. p. (Condie et al., 2000).

The simulation of marine $\delta^{18}O$ values was based on the modified water model (Fig. 5) and the fluxes defined in Table 3. The intensity of water/rock interactions at low and high temperatures (k_w, k_{up} and k_{deep}) was varied to identify possible scenarios that could explain the low $\delta^{18}O$ value of -8 ‰ postulated for the early Phanerozoic. The simulations revealed that a rapid change from a low-temperature dominated system to the current high-temperature controlled state is needed to reproduce both the low abundance of ^{18}O at the beginning of the Phanerozoic and the subsequent rapid increase in marine $\delta^{18}O$. The model run depicted in Figure 6 started with an initial value of $+7$ ‰ for the free water mass corresponding to the isotopic composition of mantle water (Hoefs, 1997). Due to the fast exchange processes, the isotopic composition changed rapidly to a steady state value defined by the relative intensity of high- and low-temperature processes (Fig. 6). The k-values for low-temperature processes (k_w, k_{up}) were increased with respect to the current values whereas the high-temperature constant k_{deep} was diminished to produce an average Precambrian $\delta^{18}O$ value of -3 ‰. This value is suggested by limestones that formed as marine precipitates during the Proterozoic and cluster around -5 ‰ PDB (Jacobsen and Kaufman, 1999; Veizer and Hoefs, 1976), reflecting both isotopically depleted seawater and some ^{18}O loss during diagenetic alteration. The kinetic constants defining the efficiency of low- and high-temperature water/rock interactions had to be changed by a factor of 3 within a rather short period preceding the Phanerozoic to produce the low $\delta^{18}O$ values of the early Cambrian. Subsequently, the k- values were adjusted to their current values to induce the decrease in marine $\delta^{18}O$ observed in the Phanerozoic carbonate data (Fig. 6).

The model implies a rapid and fundamental reorganization of the global ^{18}O cycle in the Neoproterozoic. During this period of earth's history (570–1000 My b. p.), all continental blocks were unified into one super-continent (Rodinia) that broke-up to re-assemble into a different configuration during the late

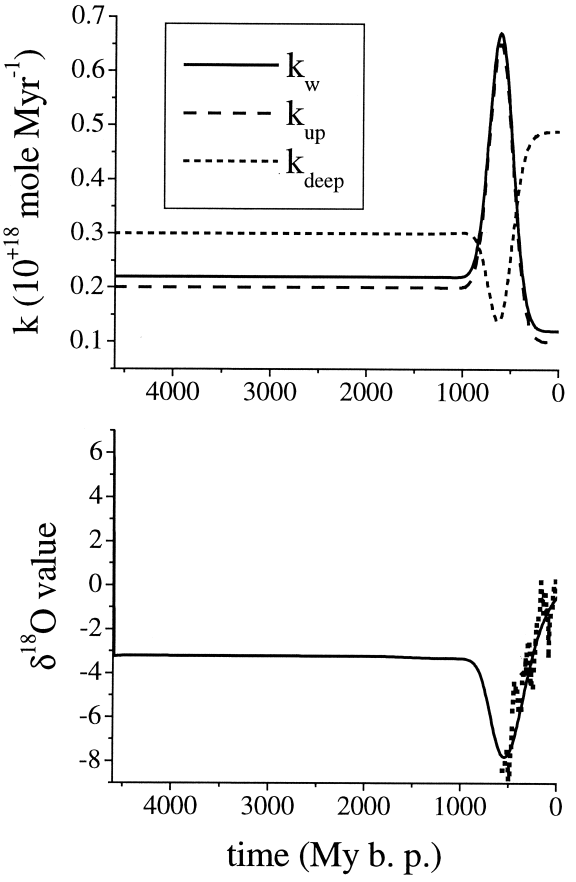

Fig. 6. Simulation of ^{18}O cycling and marine $\delta^{18}O$ values through earth's history. The upper diagram shows changes in kinetic constants, that define the intensity of isotopic exchange processes associated with continental silicate weathering (k_w) as well as low- and high-temperature seawater/rock interactions at the seafloor (k_{up}, k_{deep}). The lower diagram shows the isotopic composition of free water calculated for the scenario defined in the upper diagram and in Figure 5. Model results are plotted as solid line, while the Phanerozoic carbonate data are depicted as dots for comparison.

Neoproterozoic (Hyde et al., 2000). During super-continent periods, the rates of seafloor spreading and subduction are reduced so that the release of ^{18}O into the ocean and the atmosphere is diminished favoring the development of low marine $\delta^{18}O$ values. The break-up of large continents induces formation of massive continental flood basalts (Eldholm and Thomas, 1993). Continental volcanic deposits are highly reactive and rapidly transformed into ^{18}O-bearing clay minerals by silicate weathering processes (Gaillardet et al., 1999; Louvat and Allègre, 1997; Taylor and Lasaga, 1999; Vitousek et al., 1997). An ^{18}O depleted ocean could, thus, be produced via high rates of subaerial volcanisms and slow submarine spreading during the late Neoproterozoic. Currently, the importance of subaerial versus submarine volcanism cannot be constrained through independent data. Even the well-established Sr isotopic record is not appropriate because non-radiogenic Sr is released both through hydrothermal circulation at midocean ridges and low-temperature weathering of flood basalts (Taylor and Lasaga, 1999). The evolution of continental rift settings into submarine spreading centers during the termination of the Neoproterozoic would lead to a general shift in volcanic activity, from flood basalts on continental crust to spreading zone volcanism at submarine plate boundaries, that would support the transition from Neoproterozoic ^{18}O depletion to Phanerozoic ^{18}O enrichment because the release of ^{18}O into the ocean occurs mainly via deep circulation cells located at active spreading centers. Moreover, the ^{18}O cycling in the late Neoproterozoic ocean was affected by the pan-African orogeny. This large-scale orogeny significantly enhanced global weathering rates (Goddéris et al., 2000) and the consumption of ^{18}O, thus contributing to the Neoproterozoic ^{18}O depletion.

4.3. Simulating the Impact of Neoproterozoic Glaciations on the Marine $\delta^{18}O$ Values

Recently, Hoffman et al. (1998) proposed that the earth experienced a series of extremely severe glaciations 750 to 580 My ago. During the Vendian (575–590 My b. p.) and Sturtian (720–740 My b. p.) icehouses a significant fraction of the global water mass was locked into kilometer thick ice shields that spread into low latitudes and almost completely covered the surface of the earth (Jacobsen and Kaufman, 1999). The duration of these periods is currently under dispute, with estimates ranging from 0.35 to 1 My (Jacobsen and Kaufman, 1999) to 4 to 30 My (Hoffman et al., 1998).

The 'snowball earth' events had a strong impact on the isotopic composition of global water masses recorded in marine limestone (Hoffman et al., 1998; Jacobsen and Kaufman, 1999) that could possibly help to explain the low marine $\delta^{18}O$ values of the early Phanerozoic. During glaciations, isotopically depleted water is accumulated in ice shields whereas ^{18}O-enriched water remains in the ocean. Since an enhanced ^{18}O content in seawater shifts the balance, between ^{18}O uptake and release during water/rock interactions, towards increased ^{18}O uptake in crustal rocks, the extreme glaciations should result in a ^{18}O loss to oceanic crust and a corresponding decrease in marine $\delta^{18}O$ values. The extent of this effect depends on the isotopic contrast between ice shields and seawater, the duration of the glacial periods and the water fraction locked in ice. It is investigated with the presented ^{18}O box model taking into account the additional fluxes and boxes listed in Table 7.

The box model was modified to include additional reservoirs for ice and frozen $H_2^{18}O$. The water fluxes into and out of the ice reservoir were defined using Gauss functions (Table 7). The uptake of $H_2^{18}O$ in ice depends on the corresponding water flux, the isotopic fractionation factor, and the isotopic composition of free water that changes through time. The isotopic contrast between large continental ice shields and seawater is caused by fractionation processes associated with the evaporation of seawater, the condensation of water into clouds and the precipitation of rain and snow (Hoefs, 1997). During the last glacial, the ice shields accumulating at high latitudes were strongly depleted in ^{18}O with an average $\delta^{18}O$ value around -42 ‰ whereas the seawater was slightly enriched with an average value of approximately $+1$ ‰ (Blunier et al., 1998; Fairbanks, 1989). Thus, the overall fractionation factor was close to 0.957. In contrast, the formation of ice through freezing seawater is accompanied by a very small isotopic fractionation producing sea ice heavier than water by 2 to 3 ‰ (O'Neil, 1968). In the model, it was assumed that the ice formed during the Neopro-

Table 7. Additional parameters and model equations used in the simulation of Neoproterozoic glaciations ('snowball earth').

Parameter	Equation/Value
Change in frozen water mass	$\frac{dM_{ice}}{dt} = F_{fr} - F_{me}$
Change in frozen $H_2{}^{18}O$	$\frac{dM^{18}_{ice}}{dt} = F^{18}_{fr} - F^{ex}_{me}$
Water flux due to ice formation	$F_{fr} = A \cdot (e^{-(t-t_a)^2/2\cdot w^2} + e^{-(t-t_b)^2/2\cdot w^2})$
Water flux due to ice melting	$F_{me} = A \cdot (e^{-(t-t_a-w)^2/2\cdot w^2} + e^{-(t-t_b-w)^2/2\cdot w^2})$
Formation of frozen $H_2{}^{18}O$	$F^{18}_{fr} = \frac{\alpha_{fr} \cdot R_f}{1 + \alpha_{fr} \cdot R_f} \cdot F_{fr}$
Melting of frozen $H_2{}^{18}O$	$F^{18}_{me} = \Phi_{ice} \cdot F_{me}$
Parameter defining the intensity of glaciations	A
Parameter defining the duration of glacial periods	w
Parameters defining the timing of glaciations	t_a, t_b
Isotopic fractionation factor for ice formation	$\alpha_{fr} = 0.957$
^{18}O mole fraction in ice	$\Phi_{ice} = M^{18}_{ice}/M_{ice}$

terozoic glaciations previously passed through the hydrological cycle experiencing the same fractionation as observed during the Pleistocene glaciations. The ^{18}O flux induced by melting was set proportional to the corresponding water flux and the mole fraction of ^{18}O in melting ice, neglecting fractionation phenomena associated with the melting process. Gauss functions were used to simulate the Sturtian and Vendian icehouses. The k_w, k_{up}, k_{deep} values were tuned to reproduce the Proterozoic $\delta^{18}O$ value of -3 ‰ as in the previous simulation. The intensity and duration of glaciations were varied to explore the effect of icehouses on the isotopic composition of seawater.

Figure 7 shows that the marine $\delta^{18}O$ values were reduced by 0.5 to 1.5 ‰ when 0.1 to 0.3 $\times 10^{+24}$ g water, corresponding to 7–20% of the free water mass, were repeatedly locked in ice. In conclusion, the simulations demonstrate that severe glaciations may cause a significant ^{18}O depletion in the overall water mass (liquid and frozen). The impact of this process on the initial ^{18}O content of Phanerozoic seawater has still to be explored and depends on the duration and the extent of the Neoproterozoic icehouse events.

4.4. Reconstructing Phanerozoic Surface Temperatures

The model curve and carbonate data depicted in Figure 3 can be used to estimate temperatures assuming equilibrium calcification. The following relation was used to calculate temperatures (T in °C) from $\delta^{18}O_{PDB}$ values in marine carbonates ($CaCO_3$) and simulated seawater values ($\delta^{18}O_{SMOW}$(sw); O'Neil et al., 1969):

$$T = 16.9 - 4.38 \cdot (\delta^{18}O_{PDB}(CaCO_3) - \delta^{18}O_{SMOW}(sw)) + \\ + 0.10 \cdot (\delta^{18}O_{PDB}(CaCO_3) - \delta^{18}O_{SMOW}(sw))^2 \quad (10)$$

The resulting temperature curve, illustrated in Figure 8, should reflect the temperature at the bottom of shallow tropical seas, the habitat of benthic brachiopods that were analyzed to produce the global carbonate data set (Veizer et al., 1999). Unfortunately, the paleo-bathymetry of the different sampling sites is not well documented. Moreover, the data set contains samples from rather different paleo-latitudes. Both parameters affect the paleo-climatic interpretation of the data because temperature and isotopic composition of seawater depend on latitude and water depth.

The model curve shows a periodic change between greenhouse and icehouse conditions for most of the Phanerozoic as

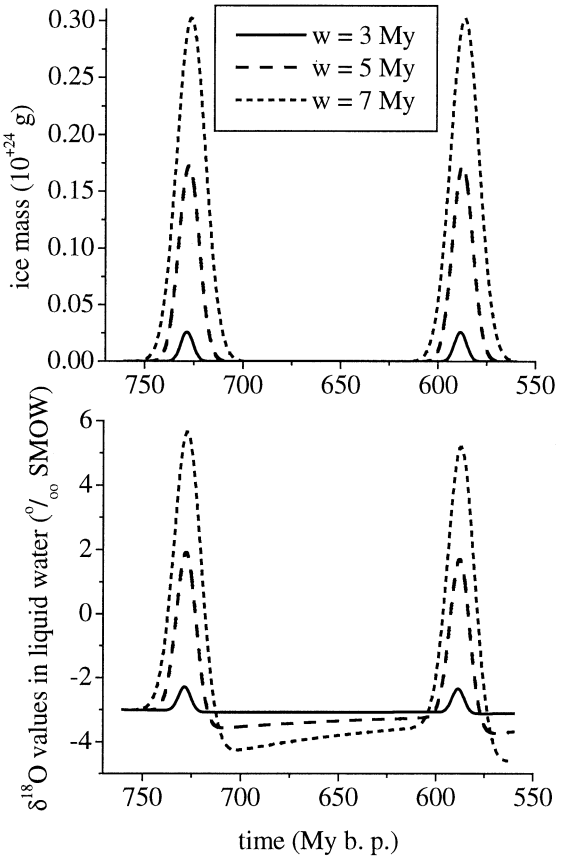

Fig. 7. Simulated change in ice mass and isotopic composition of liquid water during the late Neoproterozoic using variable intensities of ice formation (solid line: w = 3 My and A = 5 $\times 10^{+20}$ mole My^{-1}; broken line: w = 5 My and A = 2 $\times 10^{+21}$ mole My^{-1}; dotted line: w = 7 My and A = 2.5 $\times 10^{+21}$ mole My^{-1} where w defines the duration and A the intensity of glaciations).

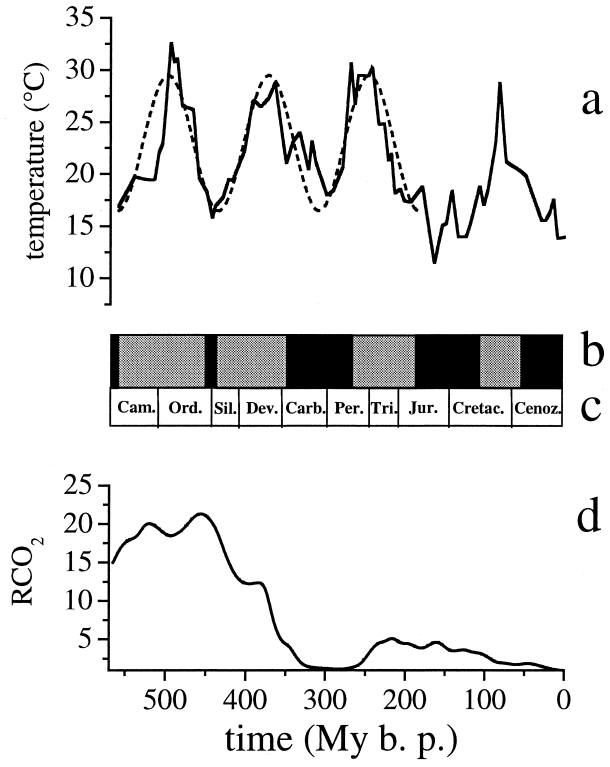

Fig. 8. Evolution of the Phanerozoic climate. *a*. Temperatures as calculated from carbonate data (Veizer et al., 1999) and the model curve depicted in Figure 3 (r_{deep} = 0.5). The thin dotted line is a sine curve fitted to the temperature data. b. Warm and cool periods as reconstructed from the distribution of glacial sediments (Frakes et al., 1992). Warm periods are marked by light-gray and cool periods by dark shading. c. Geological periods according to the time scale of Harland et al. (1990). d. Partial pressures of CO_2 in the atmosphere, standardized to the Holocene value, as simulated by Berner (1997) using the GEOCARB II model.

previously postulated by Fischer (1981). The agreement between simulated icehouse periods and cool periods, the later documented by independent geological evidence (Fig. 8), strongly supports the validity of both the carbonate isotope data and the isotope modeling. Only the low temperatures calculated for the Jurassic and early Cretaceous seem to be inconsistent with the geological evidence, but recent sediment and isotope data indicate at least periodic glaciations during the mid-Jurassic and early Cretaceous (Frakes et al., 1992; Stoll and Schrag, 1996). A simple sine function with a period of 127 My, a base line at 16.5°C, and an amplitude of 13°C describes the simulated climate fluctuations up to the onset of the Jurassic (Fig. 8). From the Jurassic to the Cenozoic, the climate pulse switched to a different pattern, a feature observed also in the geological record (Frakes et al., 1992; Huggett, 1991).

During glaciations, the $\delta^{18}O$ value of seawater is enhanced due to the accumulation of isotopically depleted ice at high latitudes. Because the magnitude and exact timing of the Phanerozoic glaciations are currently unknown, ice cap impact on seawater $\delta^{18}O$ was not considered in the model. During Pleistocene glaciations, the seawater $\delta^{18}O$ increased by about 1 ‰, corresponding to an apparent change in isotope-based temperatures by 4.4°C (Eqn. 10). Assuming a similar effect for the Phanerozoic glaciations, the low-latitude temperatures calculated for glacial periods are significantly biased to low values. Thus, the total amplitude of temperature change in low latitudes was significantly smaller than calculated. The changes in surface temperature at high-latitude as well as in global average surface water were probably more extensive than the low-latitude variations and the baseline for the global temperatures was lower than its tropical counterpart.

The most striking feature of the temperature reconstruction is the discovery of three full icehouse-greenhouse cycles with similar amplitude and periodicity (127 My), extending from the early Cambrian to the late Triassic. The evenness of this pulse is astonishing and is only revealed through the continuous isotope record. The isotope data also indicate a rapid warming at the transition from cold to warm periods and a slow decrease in surface temperatures during the transition from warm to cold periods as previously postulated by Frakes et al. (1992). A similar asymmetric change in surface temperatures is observed during the Pleistocene albeit on a much shorter time scale (Jouzel et al., 1987).

Previously, only two icehouse-greenhouse cycles with a periodicity of 250 - 300 My were assumed for the whole Phanerozoic (Fischer, 1981; 1984). As these long cycles showed a rather good correlation to changes in volcanic activity and global sea level, the climate reconstruction seemed to imply a simple climate control through partial pressures of atmospheric CO_2 controlled via tectonic and volcanic processes. In contrast, the controlling mechanisms for the much shorter periodicity seen in the new climate reconstruction (Fig. 8) remain obscure. Neither Phanerozoic sea-level curves (Hallam, 1992) nor simulated changes in atmospheric CO_2 partial pressure (Berner, 1994) are correlated with these climate cycles (Fig. 8). Nevertheless, the new climate record should be considered as an important constrain to future models of Phanerozoic climate change.

5. CONCLUSIONS

The ocean is losing water to the mantle because the subduction of water structurally bound in altered oceanic crust and serpentinized peridotites surpasses the water emission from the mantle. The total water mass decreased by 6 to 10% over the entire Phanerozoic causing a significant drop in sea-level that should be considered in the interpretation of global sea-level curves.

Mass balances and model results presented in this paper generate new and enhanced estimates of current H_2O^+-fluxes in subduction zones: The total input of structurally bound water (H_2O^+) into subduction zones amounts to $\approx 37 \times 10^{+18}$ mole My^{-1}; a major portion ($\approx 20 \times 10^{+18}$ mole My^{-1}) is generated by the reaction of seawater with sheeted dikes, gabbros and peridotites at high temperatures. Arc volcanoes release $\approx 22.5 \times 10^{+18}$ mole H_2O^+ My^{-1} into the atmosphere; the largest contribution ($\approx 20 \times 10^{+18}$ mole My^{-1}) comes from subducted sediments, altered crust and serpentinized peridotites whereas mantle degassing is of minor importance ($\approx 2.5 \times 10^{+18}$ mole My^{-1}). Approximately $17 \times 10^{+18}$ mole H_2O^+ My^{-1} are not released into ocean and atmosphere but subducted into the mantle.

The current input of ^{18}O into the ocean, through hydrother-

mal circulation at spreading centers and volcanic water emissions at subduction zones, surpasses the ^{18}O-consumption via weathering of continental rocks and seafloor alteration processes by $\approx 0.4 \times 10^{+15}$ mole ^{18}O My^{-1}.

Balance considerations and models presented in this paper strongly support the idea that seawater $\delta^{18}O$ values are not constant through time, but evolved from a depleted state during the early Cambrian to the current value. The Phanerozoic $\delta^{18}O$ increase recorded in marine carbonates (Veizer et al., 1999) can be attributed to a corresponding change in isotopic seawater composition because the rate of change in seawater $\delta^{18}O$, calculated in the model, closely follows the basic trend observed in the carbonate data.

During the Neoproterozoic, the oceanic ^{18}O budget was probably characterized by a strong ^{18}O deficit. The ^{18}O release could have been diminished during super-continent periods due to slow seafloor spreading and subduction. The uptake of ^{18}O in rocks was possibly enhanced by the weathering of subaerial volcanic deposits formed during the break-up of super-continents and by weathering of crystalline rocks exposed and eroded during the pan-African orogeny. Extensive glaciations during the late Neoproterozoic caused a further drop in seawater ^{18}O due to enhanced ^{18}O uptake in oceanic crust. The evolution of subaerial rifting into submarine spreading with extensive hydrothermal circulation might have shifted the oceanic ^{18}O balance causing a transition from an ^{18}O deficient Neoproterozoic ocean into a Phanerozoic ocean affected by strong ^{18}O inputs. Additional isotopic and geological data are needed to better constrain the nature and sequence of events at the Neoproterozoic/Phanerozoic transition.

Temperatures derived from the modeled seawater composition and from the measured carbonate data give a novel and unique record of climate change throughout the Phanerozoic. These data show that neither the icehouse nor the greenhouse conditions are the norm. The data suggest a regular and periodic alteration between warm and cold periods as the dominant feature of Phanerozoic climate. Three full icehouse-greenhouse cycles with an almost constant amplitude and a period of 127 My spanning the early Cambrian to late Triassic intervals are followed by a cool period extending from early Jurassic to early Cretaceous, a mid-Cretaceous greenhouse and a late Cenozoic icehouse.

This new climate record is not correlated with changes in tectonic activity, solar irradiation, or partial pressure of atmospheric CO_2. Thus, the climate cycles are not controlled by a single master parameter. Instead, they may be generated by the earth system itself residing in a certain state defined by its position in space, orbit parameters, palaeogeographic configuration, ecosystem organization, modes of atmospheric and oceanic circulation, as well as by the prevailing levels of volcanic and orogenic activity. Even though the mechanisms that control the climate cycles are currently not understood, the new temperature record should not be dismissed but regarded as a challenge to future models of Phanerozoic climate change.

Acknowledgments—The author would like to thank E. Suess, J. Veizer, H.-U. Schmincke, J. Phipps Morgan, Y. Goddéris and W. W. Hay for stimulating discussions. Moreover, J. Veizer provided the carbonate isotope data and encouraged the development of the ^{18}O box model. Suggestions of the associate editor S. Sheppard and constructive comments of Y. Goddéris, R. T. Gregory and an anonymous reviewer helped the author to improved the paper significantly. This work is contribution No. 1 of the Sonderforschungsbereich 574 "Volatiles and Fluids in Subduction Zones" at Kiel University.

Associate editor: S. Sheppard

REFERENCES

Agrinier P., Laverne C., and Tartarotti P. (1995a) Stable isotope ratios (oxygen, hydrogen) and the petrology of hydrothermally altered dolerites at the bottom of the sheeted dike complex of Hole 504B. *Proc. O.D.P., Sci. Res.* **13/140,** 99–106.

Agrinier P., Hékinian R., Bideau D., and Javoy M. (1995b) O and H stable isotope compositions of oceanic crust and upper mantle rocks exposed in the Hess Deep near the Galapagos Triple Junction. *Earth Planet. Sci. Lett.* **136,** 183–196.

Alt J. C. (1993) Low-temperature alteration of basalts from the Hawaiian arch, Leg 136. *Proc. O.D.P., Sci. Res.* **136,** 133–146.

Alt J. C., France-Lanord C., Castillo P., and Galy A. (1992) Low-temperature hydrothermal alteration of Jurassic ocean crust, Site 801. *Proc. O.D.P., Sci. Res.* **129,** 415–427.

Alt J. C., Honnorez J., Laverne C., and Emmermann R. (1986) Hydrothermal alteration of a 1 km section through the upper oceanic crust, Deep Sea Drilling Project Hole 504B: Mineralogy, chemistry, and evolution of seawater-basalt interactions. *J. Geophys. Res.* **91(B10),** 10309–10335.

Alt J. C. and Teagle D. A. H. (1999) The uptake of carbon during alteration of oceanic crust. *Geochim. Cosmochim. Acta* **63(10),** 1527–1536.

Alt J. C., Teagle D. A. H., Laverne C., Vanko D. A., Bach W., Honnorez J., Becker K., Ayadi M., and Pezard P. A. (1996) Ridge flank alteration of upper ocean crust in the eastern Pacific: Synthesis of results for volcanic rocks of Holes 504B and 896A. *Proc. O.D.P., Sci. Res.* **148,** 435–450.

Alt J. C., Zuleger E., and Erzinger J. (1995) Mineralogy and stable isotopic composition of the hydrothermally altered lower sheeted dike complex, Hole 504B, Leg 140. *Proc. O.D.P., Sci. Res.* **137/140,** 155–166.

Bach W., Erzinger J., Alt J. C., and Teagle D. A. H. (1996) Chemistry of the lower sheeted dike complex, Hole 504B (Leg 148): Influence of magmatic differentiation and hydrothermal alteration. *Proc. O.D.P., Sci. Res.* **148,** 39–55.

Bebout G. E. (1996) Volatile Transfer and Recycling at Convergent Margins: Mass-Balance and Insights from High-P/T Metamorphic Rocks. In *Subduction Top to Bottom* (eds. G. E. Bebout, D. W. Scholl, S. H. Kirby, and J. P. Platt) Vol. 96, pp. 179–193. American Geophysical Union.

Berner E. K. and Berner R. A. (1996) Global Environment: Water, Air and Geochemical Cycles. Prentice Hall.

Berner R. A. (1994) GEOCARB II: A revised model of atmospheric CO_2 over Phanerozoic time. *Am. J. Sci.* **294,** 56–91.

Berner R. A. (1997) The rise of plants and their effect on weathering and atmospheric CO_2. *Sci.* **276,** 544–546.

Blunier T., Chappellaz J., Schwander J., Dällenbach A., Stauffer B., Stocker T. F., Raynaud D., Jouzel J., Clausen H. B., Hammer C. U., and Johnsen S. J. (1998) Asynchrony of Antarctic and Greenland climate change during the last glacial period. *Nature.* **394,** 739–743.

Bose K. and Navreotsky A. (1998) Thermochemistry and phase equilibria of hydrous phases in the system MgO-SiO_2-H_2O: Implications for volatile transport to the mantle. *J. Geophys. Res.* **103(B5),** 9713–9719.

Bowers T. S. and Taylor H. P. Jr. (1985) An integrated chemical and stable-isotope model of the origin of midocean ridge hot-spring systems. *J. Geophys. Res.* **90(B14),** 12583–12606.

Broecker W. S. and Peng T.-H. (1982) Tracers in the Sea. Lamont-Doherty Geological Observatory, Columbia University.

Cannat M., Bideau D., and Bougault H. (1992) Serpentinized peridotites and gabbros in the Mid-Atlantic ridge axial valley at 15°37′N and 16°52′N. *Earth Planet. Sci. Lett.* **109,** 87–106.

Charlou J. L., Fouquet Y., Bougault H., Donval J. P., Etoubleau J., Jean-Babtiste P., Dapoigny A., Appriou P., and Rona P. A. (1998) Intense CH_4 plumes generated by serpentinization of ultramafic

rocks at the intersection of the 15°20′N Fracture Zone and the Mid-Atlantic Ridge. *Geochim. Cosmochim. Acta* **62(13),** 2323–2333.

Chinnery N. J., Pawley A. R., and Clark S. M. (1999) In situ observation of the formation of 10 Å phase from talc + H_2O at mantle pressures and temperatures. *Science* **286,** 940–942.

Cole D. R. and Ohmoto H. (1986) Kinetics of isotopic exchange at elevated temperatures and pressures. In *Rev. Mineral.* (eds. J. W. Valley, H. P. Taylor Jr., and J. R. O'Neil), Vol. 16, pp. 41–90. Mineralogical Society of America.

Condie K. C., Des Marais D. J., and Abbott D. (2000). Geologic evidence for a mantle superplume event at 1.9 Ga. *Geochem., Geophys., Geosys.* 1(2000GC000095).

Degens E. T. and Epstein S. (1962) Relationship between O^{18}/O^{16} ratios in coexisting carbonates, cherts, and diatomites. *Am. Pet. Geol. Bull.* **46,** 534–542.

Eldholm O. and Thomas E. (1993) Enviornmental impact of volcanic margin formation. *Earth Planet. Sci. Lett.* **117,** 319–329.

Fairbanks R. G. (1989) A 17,000-year glacio-eustatic sea level record: influence of glacial melting rates on the Younger Dryas event and deep-ocean circulation. *Nature.* **342,** 637–642.

Fischer A. G. (1981) Climatic oscillations in the biosphere. In *Biotic Crisis in Ecological and Evolutionary Time* (ed. M. H. Nitecki), pp. 103–131. Academic Press.

Fischer A. G. (1984) The two Phanerozoic supercycles. In *Catastrophes and Earth History* (eds. W. A. Berggren and J. A. van Couvering), pp. 129–150. Princeton University Press.

Frakes L. A., Francis J. E., and Syktus J. I. (1992) Climate Modes of the Phanerozoic. Cambridge University Press.

Fryer P., Pearce J. A., Stokking L. B., et al. (1990) *Proceedings of the Ocean Drilling Program, Initial Reports, Leg 125.* Ocean Drilling Program.

Gaillardet J., Dupré B., Louvat P., and Allègre C. J. (1999) Global silicate weathering and CO_2 consumption rates deduced from the chemistry of large rivers. *Chem. Geol.* **159,** 3–30.

Giggenbach W. F. (1992) Isotopic shifts in waters from geothermal and volcanic systems along convergent plate boundaries and their origin. *Earth Planet. Sci. Lett.* **113,** 495–510.

Giggenbach W. F. (1996) Chemical Composition of Volcanic Gases. In *Monitoring and Mitigation of Volcanic Hazards* (ed. R. Scosper and R. I. Tilling), pp. 221–256. Springer-Verlag.

Goddéris Y., François L., and Veizer J. (2000). Paleozoic carbon cycle. *Earth Planet. Sci. Lett.* (submitted)

Goddéris Y. and Veizer J. (2000). Tectonic control of chemical and isotopic composition of ancient oceans: the impact of continental growth. *Am. J. Sci.* **300,** 437–461.

Gregory R. T. (1991) Oxygen isotope history of seawater revisited: timescales for boundary event changes in the oxygen isotope composition of seawater. In *Stable Isotope geochemistry: A Tribute to Samuel Epstein.* (eds. H. P. Taylor, J. R. O'Neil, and I. R. Kaplan) Geochem. Soc. Spec. Publ. 3, pp. 65–76.

Gregory R. T. and Taylor H. P. (1981) An oxygen isotope profile in a section of Cretaceous oceanic crust, Samail Ophiolite, Oman: Evidence for $\delta^{18}O$ buffering of the oceans by deep (>5 km) seawater hydrothermal circulation at mid-ocean ridges. *J. Geophys. Res.* **86(B4),** 2737–2755.

Hales B. and Emerson S. (1997) Evidence in support of first-order dissolution kinetics of calcite in seawater. *Earth Planet. Sci. Lett.* **148,** 317–327.

Hallam A. (1992) Phanerozoic Sea-Level Changes. Columbia University Press.

Harland W. B., Armstrong R. L., Cox A. V., Craig L. E., Smith A. G., and Smith D. G. (1990) A Geologic Time Scale. Cambridge University Press.

Hart S. R., Blusztajn J., Dick H. J. B., Meyer P. S., and Muehlenbachs K. (1999) The fingerprint of seawater circulation in a 500-meter section of ocean crust gabbros. *Geochim. Cosmochim. Acta* **63(23/24),** 4059–4080.

Hoefs J. (1997) Stable Isotope Geochemistry, 4th edition. Springer-Verlag.

Hoffman P. F., Kaufman A. J., Halverson G. P., and Schrag D. P. (1998) A Neoproterozoic snowball earth. *Science.* **281,** 1342–1346.

Holland H. D. (1984) The Chemical Evolution of the Atmosphere and Oceans. Princeton University Press.

Huggett R. J. (1991) Climate, Earth Processes and Earth History. Springer-Verlag.

Hurd D. C. (1972) Factors affecting solution rate of biogenic opal in seawater. *Earth Planet. Sci. Lett.* **15(4),** 411–417.

Hyde W. T., Crowley T. J., Baum S. K., and Eltier R. (2000) Neoproterozoic 'snowball Earth' simulations with a coupled climate/ice-sheeet model. *Nature.* **405,** 425–429.

Ito E., Harris D. M., and Anderson A. T. (1983) Alteration of oceanic crust and geologic cycling of chlorine and water. *Geochim. Cosmochim. Acta* **47,** 1613–1624.

Jacobsen S. B., and Kaufman A. J. (1999) The Sr, C and O isotopic evolution of Neoproterozoic seawater. *Chem. Geol.* **161,** 37–57.

Javoy M., and Pineau F. (1991) The volatiles record of a "popping" rock from the Mid-Atlantic Ridge at 14°N: chemical and isotopic composition and isotopic composition of gas trapped in the vesicles. *Earth Planet. Sci. Lett.* **107,** 598–611.

Jean-Baptiste P., Charlou J. L., and Stievenard M. (1997) Oxygen isotope study of mid-ocean ridge hydrothermal fluids: Implication for the oxygen-18 budget of the ocean. *Geochim. Cosmochim. Acta* **61(13),** 2669–2677.

Jouzel J., Lorius C., Petit J. R., Genthon C., Barkov N. I., Kotlayakov V. M., and Petrov V. M. (1987) Vostock ice-core: a continuous isotope temperature record over the last climatic cycle (160,000 years). *Nature.* **329,** 403–408.

Kadko D., Baross J., and Alt J. (1995) The Magnitude and Global Implications of Hydrothermal Flux. In *Seafloor Hydrothermal Systems: Physical, Chemical, Biological, and Geological Interactions* (eds. S. E. Humphris, R. A. Zierenberg, L. S. Mullineaux, and R. E. Thomson), pp. 446–466. AGU.

Kastner M., Elderfield H., Jenkins W. J., Gieskes J. M., and Gamo T. (1993) Geochemical and isotopic evidence for fluid flow in the Western Nankai Subduction Zone, Japan. *Proc. O.D.P., Sci. Res.* **131,** 397–413.

Kastner M., Elderfield H., Martin J. B., Suess E., Kvenvolden K. A., and Garrison R. E. (1990) Diagenesis and interstitial-water chemistry at the Peruvian continental margin—Major constituents and strontium isotopes. *Proc. O.D.P.* **112,** 413–440.

Kelley D. S. (1996) Methane-rich fluids in the oceanic crust. *J. Geophys. Res.* **101,** 2943–2962.

Kempton P. D., Hawesworth C. J., and Fowler M. (1991) Geochemistry and isotopic composition of gabbros from layer 3 of the Indian Ocean crust, Hole 735B. *Proc. O.D.P., Sci. Res.* **118,** 127–143.

Land L. S. (1995) Comment on "Oxygen and carbon isotopic composition of Ordovician brachiopods: Implications for coeval seawater" by H. Quing and J. Veizer. *Geochim. Cosmochim. Acta* **59(13),** 2843–2844.

Land L. S. and Lynch F. L. (1999) Reply to "Comment on '$\delta^{18}O$ values of mudrocks: More evidence for an ^{18}O buffered ocean'". *Geochim. Cosmochim. Acta* **63(15),** 2213.

Le Cloarec M.-F. and Marty B. (1991) Volatile fluxes from volcanoes. *Terra Nova.* **3,** 17–27.

Lécuyer C. and Allemand P. (1999) Modelling of oxygen isotope evolution of seawater: Implications for the climate interpretation of the $\delta^{18}O$ of marine sediments. *Geochim. Cosmochim. Acta* **63(3/4),** 351–361.

Li Y.-H. (1972) Geochemical mass balance among lithosphere, hydrosphere, and atmosphere. *Am. J. Sci.* **272,** 119–137.

Liu J. and Bohlen S. R. (1996) Stability of hydrous phases in subducting oceanic crust. *Earth Planet. Sci. Lett.* **143,** 161–171.

Louvat P. and Allègre C. J. (1997) Present denudation rates on the island of Réunion determined by river geochemistry: Basalt weathering and mass budget between chemical and mechanical erosions. *Geochim. Cosmochim. Acta* **61(17),** 3645–3669.

Lupton J. E., Baker E. T., and Massoth G. J. (1989) Variable ^3He/heat ratios in submarine hydrothermal systems: evidence from two plumes over the Juan de Fuca Ridge. *Nature.* **337,** 161–164.

Mibe K., Fujii T., and Yasuda A. (1999) Control of the location of the volcanic front in island arcs by aqueous fluid connectivity in the mantle wedge. *Nature.* **401,** 259–262.

Moore J. C. and Vrolijk P. (1992) Fluids in accretionary prisms. *Rev. Geophys.* **30,** 113–135.

Moore J. G. (1970) Water content of basalt erupted on the ocean floor. *Contrib. Miner. Petrol.* **28,** 272–279.

Muehlenbachs K. (1986) Alteration of the oceanic crust and the ^{18}O history of seawater. In *Stable Isotopes in High Temperature Geological Processes* (eds. J. W. Valley, H. P. Taylor Jr., and J. R. O'Neil) Vol. 16, pp. 425–444. Mineralogical Society of America.

Muehlenbachs K. (1998) The oxygen isotopic composition of the oceans, sediments and the seafloor. *Chem. Geol.* **145,** 263–273.

Muehlenbachs K. and Clayton R. N. (1976) Oxygen isotope composition of the oceanic crust and its bearing on seawater. *J. Geophys. Res.* **81(23),** 4365–4369.

Mysen B. O. and Acton M. (1999) Water in H_2O-saturated magma-fluid systems: Solubility behavior in K_2O-Al_2O_3-SiO_2-H_2O to 2.0 GPa and 1300°C. *Geochim. Cosmochim. Acta* **63(22),** 3799–3815.

O'Neil J. R. (1968) Hydrogen and oxygen fractionation between ice and water. *J. Phys. Chem.* **72,** 3683–3684.

O'Neil J. R., Clayton R. N., and Mayeda T. K. (1969) Oxygen isotope fractionation in divalent metal carbonates. *J. Chem. Phys.* **51,** 5547–5558.

Ono S. (1998) Stability limits of hydrous minerals in sediment and mid-ocean ridge basalt compositions: Implications for water transport in subduction zones. *J. Geophys. Res.* **103(B5),** 18253–18267.

Peacock S. M. (1990) Fluid processes in subduction zones. *Science* **248,** 329–337.

Perry E. C. and Tan F. C. (1972) Significance of oxygen and carbon isotope variations in early Precambrian cherts and carbonate rocks of southern Africa. *Geol. Soc. Am. Bull.* **83,** 647–664.

Phipps Morgan J. (1998) Thermal and rare gas evolution of the mantle. *Chem. Geol.* **145,** 431–445.

Plank T. and Langmuir C. H. (1998) The chemical composition of subducting sediment and its consequences for the crust and mantle. *Chem. Geol.* **145,** 325–394.

Press W. H., Teukolsky S. A., Vetterling W. T., and Flannnery B. P. (1992) Numerical Recipes. Cambridge University Press.

Robinson P. T., Dick H. J. B., and von Herzen R. (1991) Metamorphism and alteration in oceanic layer 3: Hole 735B. *Proc. O.D.P., Sci. Res.* **118,** 541–549.

Sano Y. and Williams S. N. (1996) Fluxes of mantle and subducted carbon along convergent plate boundaries. *Geophys. Res. Lett.* **23(20),** 2749–2752.

Schmidt M. W. and Poli S. (1998) Experimentally based water budgets for dehydrating slabs and consequences for arc magma generation. *Earth Planet. Sci. Lett.* **163,** 361–379.

Schmincke H.-U. (2000) Vulkanismus. Wissenschaftliche Buchgesellschaft.

Seyfried W. F. and Dibble W. E. Jr. (1980) Seawater-peridotite interaction at 300°C and 500 bars: implications for the origin of oceanic serpentinites. *Geochim. Cosmochim. Acta.* **44,** 309–321.

Shanks W. C. III., Böhlke J. K., and Seal R. R. II. (1995) Stable isotopes in Mid-Ocean Ridge Hydrothermal Systems: Interactions between Fluids, Minerals, and Organisms. In *Seafloor Hydrothermal Systems: Physical, Chemical, Biological, and Geological Interactions* (eds. S. E. Humphris, R. A. Zierenberg, L. S. Mullineaux, and R. E. Thomsen), pp. 194–221. AGU.

Snow J. E. and Dick H. J. B. (1995) Pervasive magnesium loss by marine weathering of peridotite. *Geochim. Cosmochim. Acta* **59(20),** 4219–4235.

Stakes D., Mével C., Cannat M., and Chaput T. (1991) Metamorphic stratigraphy of hole 735B. *Proc. O.D.P., Sci. Res.* **118,** 153–180.

Staudigel H., Davies G. R., Hart S. R., Marchant K. M., and Smith B. M. (1995) Large scale isotopic Sr, Nd and O isotopic anatomy of altered oceanic crust: DSDP/ODP sites 417/418. *Earth Planet. Sci. Lett.* **130,** 169–185.

Staudigel H., Plank T., White B., and Schmincke H.-U. (1996) Geochemical Fluxes During Seafloor Alteration of the Basaltic Upper Oceanic Crust: DSDP Sites 417 and 418. In *Subduction Top to Bottom* (eds. G. E. Bebout, D. W. Scholl, S. H. Kirby, and J. P. Platt) Vol. 96, pp. 19–38. AGU.

Staudigel H. R., Hart S. R., Schmincke H. U., and Smith B. M. (1990) Cretaceous ocean crust at DSDP Sites 417 and 418: Carbon uptake from weathering versus loss by magmatic outgassing. *Geochim. Cosmochim. Acta* **53,** 3091–3094.

Stoll H. M. and Schrag D. P. (1996) Evidence for glacial control of rapid sea level changes in the early Cretaceous. *Science* **272,** 1771–1774.

Taylor A. S. and Lasaga A. C. (1999) The role of basalt weathering in the Sr isotope budget of the oceans. *Chem. Geol.* **161,** 199–214.

Taylor S. R. and McLennan S. M. (1995) The geochemical evolution of the continental crust. *Rev. Geophys.* **33(2),** 241–265.

Thompson A. B. (1992) Water in the earth's upper mantle. *Nature* **358,** 295–302.

Torgersen T. (1989) Terrestrial helium degassing fluxes and the atmospheric helium budget: Implications with respect to the degassing processes of continental crust. *Chem. Geol.* **79,** 1–14.

Turekian K. K. and Wedepohl K. H. (1961) Distribution of the elements in some major units of the Earth's crust. *Geol. Soc. Am. Bull.* **72,** 175–192.

Ulmer P. and Trommersdorff V. (1995) Serpentine stability to mantle depths and subduction-related magmatism. *Science* **268,** 858–861.

Vanko D. A. and Stakes D. S. (1991) Fluids in oceanic layer 3: Evidence from veined rocks, Hole 735B, southwest Indian Ridge. *Proc. O.D.P., Sci. Res.* **118,** 181–215.

Veizer J. (1995) Reply to the Comment by L. S. Land on "Oxygen and carbon isotopic composition of Ordovician brachiopods: Implications for coeval seawater." *Geochim. Cosmochim. Acta* **59(13),** 2845–2846.

Veizer J. (1999) Comment on "$\delta^{18}O$ values of mudrocks: More evidence for an ^{18}O buffered ocean" by L. S. Land and F. L. Lynch, Jr. *Geochim. Cosmochim. Acta* **63(15),** 2311–2312.

Veizer J., Ala D., Azmy K., Bruckschen P., Buhl D., Bruhn F., Carden G. A. F., Diener A., Ebneth S., Goddéris Y., Jasper T., Korte C., Pawellek F., Podlaha O. G., and Strauss H. (1999) $^{87}Sr/^{86}Sr$, $\delta^{13}C$, and $\delta^{18}O$ evolution of Phanerozoic seawater. *Chem. Geol.* **161,** 59–88.

Veizer J., Bruckschen P., Pawellek F., Diener A., Podlaha O. G., Carden G. A. F., Jasper T., Korte C., Strauss H., Azmy K., and Ala D. (1997) Oxygen isotope evolution of Phanerozoic seawater. *Palaeogeo., Palaeoclim., Palaeoeco.* **132,** 159–172.

Veizer J., Goddéris Y.-F., and François L. M. (2000). Evidence for decoupling of atmospheric CO_2 and global climate during the Phanerozoic eon. *Nature.* **408,** 698–701.

Veizer J. and Hoefs J. (1976) The nature of $^{18}O/^{16}O$ and $^{13}C/^{12}C$ secular trends in sedimentary carbonates. *Geochim. Cosmochim. Acta* **40,** 1387–1395.

Veizer J. and Jansen S. L. (1979) Basement and sedimentary recycling and continental evolution. *J. Geol.* **87,** 341–370.

Vitousek P. M., Chadwick O. A., Crews T. E., Fownes J. H., Hendricks D. M., and Herbert D. (1997) Soil and ecosystem development across the Hawaiian Islands. *GSA Today.* **7(9),** 1–8.

Von Huene R. and Scholl D. W. (1991) Observations at convergent margins concerning sediment subduction, subduction erosion, and the growth of continental crust. *Rev. Geophys.* **29(3),** 279–316.

Walker J. C. G. and Lohmann K. C. (1989) Why the oxygen isotopic composition of sea water changes with time. *Geophys. Res. Lett.* **16(4),** 323–326.

Watson E. B. and Lupulescu A. (1993) Aqueous fluid connectivity and chemical transport in clinopyroxene-rich rocks. *Earth Planet. Sci. Lett.* **117,** 279–294.